Human occupation of the semi-arid grasslands of South Africa during MIS 4: New archaeological and paleoecological evidence from Lovedale, Free State

Kristen Wroth, Chantal Tribolo, C. Britt Bousman, Liora Kolska Horwitz, Lloyd Rossouw, Christopher E Miller, Michael B Toffolo

Quaternary Science Reviews 283 (2022) 107455

Human occupation of the semi-arid grasslands of South Africa during MIS 4: New archaeological and paleoecological evidence from Lovedale, Free State

Kristen Wroth [a, *], Chantal Tribolo [b], C. Britt Bousman [c], Liora Kolska Horwitz [d], Lloyd Rossouw [e, f], Christopher E. Miller [a, g], Michael B. Toffolo [h]

[a] Institut für Naturwissenschaftliche Archa€ologie and Senckenberg Centre for Human Evolution and Paleoenvironment (HEP), Eberhard-Karls-Universita€t Tübingen, Ho€lderlinstraße 12, 72070, Tübingen, Germany
[b] CNRS, UMR 6034 Arch,eosciences Bordeaux, Universit,e Bordeaux Montaigne, 8 Esplanade des Antilles, 33607, Pessac, France
[c] Department of Anthropology, Texas State University, 601 University Drive, San Marcos, TX, 78666-4684, USA
[d] National Natural History Collections, Hebrew University of Jerusalem, Berman Building, E. Safra-Givat Ram Campus, 91904, Jerusalem, Israel
[e] Florisbad Quaternary Research Department, National Museum Bloemfontein, 36 Aliwal Street, 9300, Bloemfontein, South Africa
[f] Department of Plant Sciences, University of the Free State, 205 Nelson Mandela Drive, 9301, Bloemfontein, South Africa
[g] SFF Centre for Early Sapiens Behaviour (SapienCE), Department of Archaeology, History, Cultural Studies and Religion, University of Bergen, PO Box 7800, 5020, Bergen, Norway
[h] Arch,eosciences Bordeaux, UMR 6034 CNRS, Universit,e Bordeaux Montaigne, 8 Esplanade des Antilles, 33607, Pessac, France

Keywords:
South Africa
Middle Stone Age
Florisian Phytolith
FTIR
Micromorphology
Luminescence
Paleoenvironment
Paleoecology Alluvial

a b s t r a c t

Marine Isotope Stage (MIS) 5 and 4 are periods of major cultural innovations in the Middle Stone Age (MSA) of southern Africa. While extensive data is available for the coast, far less is known about the interior, in particular its central plateau. This is likely due to the large geographic extent of this area and a general paucity of caves and rock shelters that can provide long stratigraphic sequences and environ- mental records. The lack of information and systematic research has hindered our understanding of regional variation and patterns of human dispersal within the subcontinent. Our research at the open-air MSA site of Lovedale situated on the Modder River addresses this issue. Using sediment micromor- phology, infrared spectroscopy of bones and sediments, phytolith and faunal analyses, as well as luminescence dating, we have reconstructed the evolution of paleoenvironments in this region at specific points over the last ~80,000 years. Our results help contextualize human occupation and hunting stra- tegies associated with a pre-Howiesons Poort technology that occurred in a wetland environment during a short-lived warm, dry period dated to ~70 ka. These results show that humans settled the grasslands of the central interior at the onset of MIS 4 and confirm the importance of wetlands in human subsistence strategies, especially in times of climatic stress.

1. Introduction

In southern Africa, Marine Isotope Stage (MIS) 5 (~130e71 ka) and MIS 4 (~71e57 ka; Lisiecki and Raymo, 2005) are important periods in the evolution of anatomically modern humans, charac- terized by many cultural and technological innovations. These include the Still Bay (SB) and Howiesons Poort (HP) lithic technocomplexes of the Middle Stone Age (MSA) (Henshilwood, 2012; Henshilwood and Dubreuil, 2011; Jacobs and Roberts, 2017; Tribolo et al., 2013; Wadley, 2015), extensive evidence of symbolic behavior (d'Errico et al., 2005; Henshilwood et al., 2011; Henshilwood et al., 2002; Texier et al., 2010), habitual heat treatment of stone tools (Brown et al., 2009; Schmidt et al., 2013), development of pressure flaking (Mourre et al., 2010; Villa et al., 2009), increased use of bone tools (Backwell et al., 2008; d'Errico et al., 2012; d'Errico and Henshilwood, 2007), development of compound adhesives for

* Corresponding author.
E-mail address: kristen-nicole.wroth@uni-tuebingen.de (K. Wroth).

tool hafting (Lombard, 2007; Wadley, 2013; Wadley et al., 2009), and the appearance of bow-and-arrow technology (Backwell et al., 2018; Lombard and Phillipson, 2010). These innovations emerged against a backdrop of marked climate change that likely played a role in their appearance, even as the climate patterns varied considerably over time and across the subcontinent, with alterna- tions of wet and dry events at the millennial timescale (d'Errico et al., 2017).

The second half of MIS 5 and the onset of MIS 4, which coincided with the development of the SB cultural tradition (Jacobs and Roberts, 2017; Tribolo et al., 2013), featured a humid climate along the western and southern coasts of South Africa (Chase, 2010; Scott and Neumann, 2018 and references therein), whereas the eastern coast experienced pulses of arid and humid conditions (Hahn et al., 2021; Ziegler et al., 2013). The climate became drier and colder during MIS 4, marking a general trend towards increased aridity (d'Errico et al., 2017; Woillez et al., 2014). Much of this ev- idence comes from marine records extracted from ocean sediment cores, which have been linked to cave and rock shelter sites with deep, well-stratified deposits that include terrestrial environ- mental records (e.g., Bar-Matthews et al., 2010; Bruch et al., 2012; Carr et al., 2016; Chase and Meadows, 2007; Clark and Kandel, 2013; Dewar and Stewart, 2016; Urrego et al., 2015). Other re- gions also show varied climatic conditions. For example, lakes and archaeological sites in the central Kalahari Basin feature humid events during MIS 4 (Burrough, 2016; Burrough et al., 2009a, 2009b; Robbins et al., 2016), whereas the southern Kalahari ap- pears to be drier (e.g., Lukich and Ecker, 2022; Telfer and Thomas, 2007).

Within this picture of environmental variability, the interior of South Africa, beyond the Great Escarpment, is still relatively un- derrepresented, with significantly fewer terrestrial records in comparison to other parts of the subcontinent (Lukich and Ecker, 2022; Scott and Neumann, 2018). This may partly be attributed to the immense size of the central interior and the fact that, with very few exceptions, most archaeological sites here are open-air sites that are not readily visible in the landscape and require large-scale surveys to be detected (e.g., Sampson et al., 2015). Moreover, these open-air sites are found within active sedimentary environments that may completely obliterate or obscure traces of human occu- pation, making them more difficult to identify (Kent and Scholtz, 2003). Consequently, only a small number of MSA sites are known, and of these, only a fraction have been accurately dated e with few reaching back to MIS 4 or earlier (Mackay et al., 2014; Wurz, 2016). Even fewer have been characterized from a paleo- environmental perspective (e.g., Florisbad: Brink, 1987; Brink et al., 2016; Brink and Henderson, 2001; Kuman et al., 1999; Scott et al., 2019; Toffolo et al., 2017; Wonderwerk: Chazan et al., 2020; Ecker et al., 2018; Kathu Pan: Lukich et al., 2020; Lukich et al., 2019; Baden Baden: van Aardt et al., 2016; Ga-Mohana Hill North: Wilkins et al., 2020; Wilkins et al., 2021).

This paucity of evidence has hindered a proper assessment of local environmental variability, human paleoecology, and dispersal within the subcontinent, to the point that we are currently unable to formulate a narrative of local population dynamics in the interior during the MSA (Sealy, 2016). In this context, one particularly understudied region of the South African interior is the Free State Province (henceforth Free State), between the Vaal and Orange Rivers (Fig. 1). Its Grassland Biome, today dissected by sporadic rivers and punctuated by springs and seasonally dry lakes (pans), was characterized by exceptionally productive grasslands and wetlands at various stages during the Middle and Late Pleistocene, supporting large game populations that provided humans with a resource-rich environment (Brink, 2016). The best example of this setting is Florisbad, a spring site at the margin of a pan in the western Free State that has produced the partial cranium of an archaic *Homo sapiens* dated to 259 ± 35 ka (Bruner and Lombard, 2020; Clarke, 1985; Grün et al., 1996), early MSA and pre-HP lithic assemblages including an intact occupation surface dated to 121 ± 6 ka (Brink and Henderson, 2001; Henderson, 2001; Kuman et al., 1999), and the type faunal assemblage of the Florisian Land Mammal Age (LMA; between ~780 and 578 ka, and ~10 ka) (Brink, 1987, 1988, 2016; Brink and Lee-Thorp, 1992; Lacruz et al., 2002), currently termed Late Naivashan (Van Couvering and Delson, 2020). The deep stratigraphic sequence at Florisbad, spanning the last ~300,000 years, has allowed paleoenvironmental re- constructions based on sediments (Toffolo et al., 2017), pollen (Scott et al., 2019), phytoliths (Scott and Rossouw, 2005), and stable isotopes of herbivore tooth enamel (Codron et al., 2008). However, Florisbad lacks occupations that can be linked to MIS 4, and remains an isolated case in the Free State.

Other spring and pan sites in the central interior have yielded well-dated pollen sequences covering portions of the Late Pleisto- cene, but no MSA artifacts (Scott and Neumann, 2018; Scott et al., 2022). In contrast, several MSA sites excavated in the last century were not dated by absolute means, such as Orangia along the Or- ange River (Sampson, 1968), Kranskraal along the Modder River (van Hoepen, 1932), and the Vlakkraal spring south of Florisbad (Wells et al., 1942). Other sites have produced only a limited spectrum of environmental proxies due to preservation issues, like Rose Cottage Cave in the eastern Free State (Lennox and Wadley, 2022). The latter, located at the foot of the Maloti-Drakensberg range close to the Lesotho border, is the only site in the Free State featuring early MIS 4 occupations (Pienaar et al., 2008; Soriano et al., 2007; Valladas et al., 2005). Recent research at Erfkroon, an extensive alluvial site on the right bank of the Modder River, documented a series of well-dated, pre- and post-HP occupations in association with faunal remains representative of the Grassland Biome, although none of these falls within MIS 4 (Bousman et al., in press; Brink et al., 2016; Churchill et al., 2000). Consequently, it is difficult to understand the cultural connections between the cen- tral interior and the SB and HP sites on the coast.

In order to address the lacuna regarding MIS 4 human paleo- ecology in the grasslands of the Free State, we focused our attention on open-air erosional gullies, or 'dongas', a common feature in local river terraces. Dongas expose Pleistocene sedimentary sequences that often contain artifacts and fossils, which become apparent in an otherwise flat landscape where buried sites are invisible to remote sensing and to the naked eye (Brink et al., 2016; Churchill et al., 2000). At Lovedale, 10 km upstream of Erfkroon, we exca- vated an MSA site within a small donga that produced a rich lithic assemblage of pre-HP technology. Here we demonstrate that by using a multi-analytical approach including micromorphology of sediments, infrared spectroscopy of sediments and fauna, phytolith analysis, faunal analyses, and luminescence dating, we can recon- struct the evolution of paleoenvironments at specific points over the last ~80,000 years and provide a context for human occupation. These data show the importance of the grasslands of the central interior of South Africa, a key region for human evolution at the crossroads between the coast and the Kalahari Basin.

1.1. Site description

Lovedale is located in the western Free State on the left bank of the Modder River, in the Petrusburg District ($28^{o}54^{0}2.35^{00}$S; $25^{o}41^{0}7.69^{00}$E; 1220 m a.s.l.) (Fig. 2). In this area, which is part of the Highveld, the Modder River flows westwards in a meandering fashion through the Free State 'panfield', a region characterized by many seasonally dry lakes or pans that are thought to be remnants of a paleodrainage disrupted by tectonic activity (Barker, 2011;

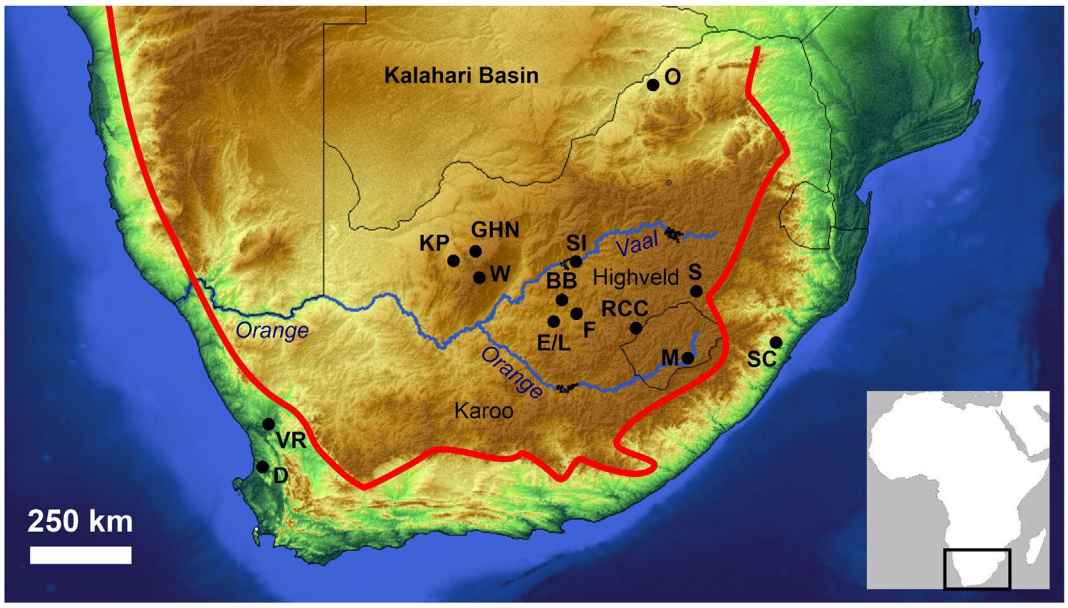

Fig. 1. Map of southern Africa showing the location of archaeological sites mentioned in the text, including Baden-Baden (BB), Diepkloof (D), Erfkroon/Lovedale (E/L), Florisbad (F), Ga-Mohana Hill North (GHN), Kathu Pan (KP), Melikane (M), Olieboompoort (O), Rose Cottage Cave (RCC), Sunnyside (S), Sibudu Cave (SC), Sheppard Island (SI), Varsche Rivier 003 (VR), and Wonderwerk (W). Red line indicates the Great Escarpment, the topographic feature that separates the higher inland plateau from the lower coastal zone. (For inter- pretation of the references to color in this figure legend, the reader is referred to the Web version of this article.)

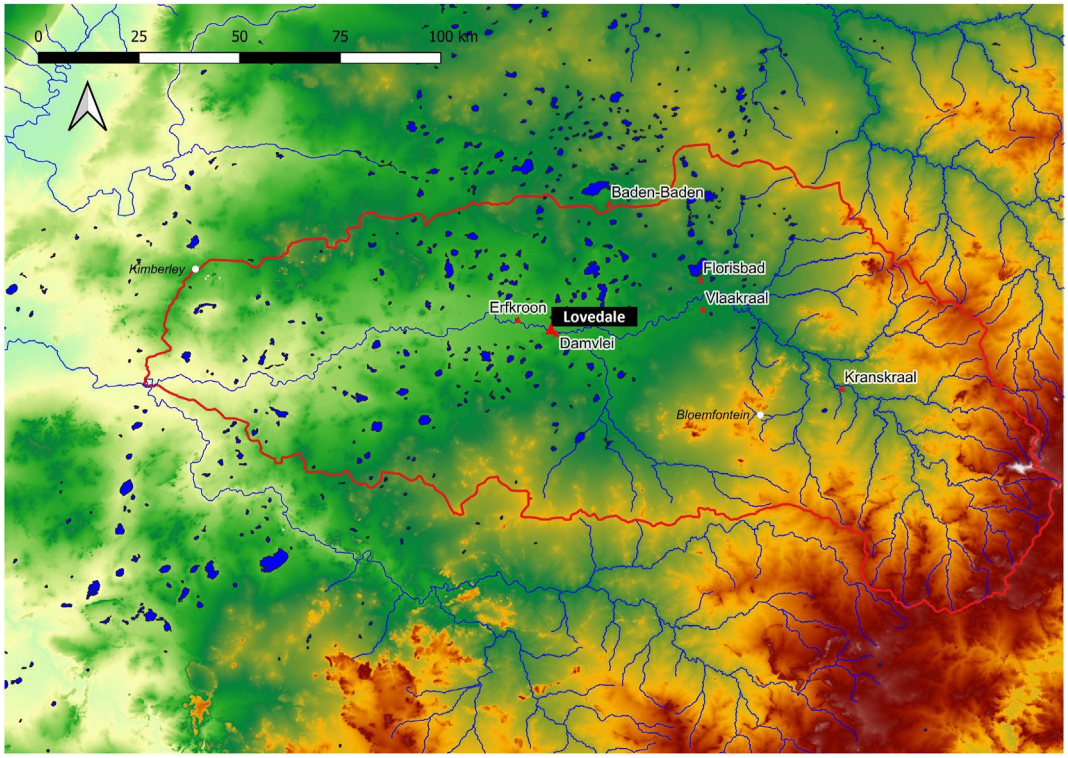

Fig. 2. Map of the western Free State showing the Modder River catchment area (red line), the study site and other archaeological sites mentioned in the text (red triangles). Pans are marked in blue. (For interpretation of the references to color in this figure legend, the reader is referred to the Web version of this article.)

Grobler et al., 1988; Marshall and Harmse, 1992). Over time, the Modder River incised its valley fill and created a succession of terraces of different ages featuring channel deposits, which vary from coarse gravel to silty sand, and overbank deposits rich in sandy clay with various degrees of pedogenic alteration (Tooth et al., 2013). This is a semi-arid, open grassland that belongs to the Grassland Biome and includes the Western Free State Clay Grassland, also known as dry *Cymbopogon-Themeda* veld, which receives 450e530 mm of annual precipitation concentrated in the spring and summer (October to March) (Acocks, 1975; Mucina and

Rutherford, 2006). Rainfall is often associated with thunderstorms, which favor high surface run-off and thus extensive erosion. This process results in the formation of dongas cutting down river ter- races. Lovedale is found in a relatively small donga, ~200,000 m^2 in surface extent, where gullies and crests dominate the landscape (Fig. 3). The gullies drain surface waters into the river through a break in the alluvial levee, which is covered by a thick canopy of vegetation and stands about 6 m above the donga floor. A large dolerite hill 100 m upstream may have facilitated the preservation of the ancient Lovedale terrace and its MSA artifacts by preventing the formation of a meander (King, 1963). In support of this inter- pretation, another site excavated by our team immediately up- stream of the dolerite hill in the Damvlei donga has produced only Later Stone Age (LSA) artifacts and sediments.

Dolerite is the product of Jurassic volcanic activity and its intrusion into Permian shale, the local bedrock (Tierberg Forma- tion, Ecca Group, Karoo Supergroup), generated outcrops of baked shale, or hornfels, by contact metamorphism (Loock and Grobler, 1988). This rock, also known as lydianite, was extensively quar- ried by MSA people in the region for stone tool production (Sampson, 1968). Hornfels outcrops occur on the eastern side of the dolerite hill between Lovedale and Damvlei, but the quality of its conchoidal fracture is poor and thus not suitable for knapping. However, rounded hornfels cobbles of excellent knapping quality are found in the Modder River.

1.2. Research history

The Lovedale site was discovered by G. Trower in 2011 during a survey of the upper Modder River valley led by J. Brink (National Museum Bloemfontein) and C. B. Bousman (Texas State University) (Trower, 2010). At this locality, stone artifacts with a gray patina and showing features typical of MSA technology were found at the bottom of erosional gullies, together with faunal remains of un- known age. A small number of LSA stone artifacts with brown patina were found at the top of the sedimentary sequence, where the plant cover is still preserved. Lovedale was surveyed again in 2014 by J. Brink, C. B. Bousman and M. Toffolo. In 2018, M. Toffolo identified the artifact-bearing layer out of which the MSA artifacts were eroding. No other sedimentary units in the donga contain MSA cultural material. Excavations began in 2019 with the aim of reconstructing the formation processes of the site, its paleoenvir- onmental context, and the nature of human occupation.

2. Materials and methods

2.1. Excavation strategy

Three areas of the site were investigated. Area A exhibits an almost complete stratigraphic sequence down to the donga bottom, except for the Holocene sediments at the top that are partially eroded. As this area was surrounded by a rich artifact scatter, it was selected for excavation (Fig. 4). A grid system anchored to a local beacon was laid out and square trenches (1 x 1 m) were randomly selected for excavation. Sediments were excavated in arbitrary 10 cm spits, down to a depth of 60 cm and sieved through a 4 mm mesh. In addition, the erosional profile of the donga in Area A was cut back to expose the full stratigraphic sequence and provide the framework for absolute dating ('dating profile') (Fig. 4). The north slope of Area A features a small remnant of older stratigraphy that dips under Area A and pinches out towards the dating profile. It includes a gravel layer rich in vertebrate fauna that was excavated separately (Fig. 4). Malacofauna crops out repeatedly in point-bar deposits between Area A and the current river channel. A few meters to the south of Area A, the sediment under the preserved plant cover provided the missing Holocene part of the stratigraphic sequence. Area B, which lies 10 m to the east of Area A, was probed but immediately abandoned due to its heavily cemented sediments and the absence of part of the artifact layer. Area C lies about 100 m to the west of Area A and produced a large collection of surface

Fig. 3. General view of the Lovedale donga, looking east. The main excavation area is located in the center of the photo.

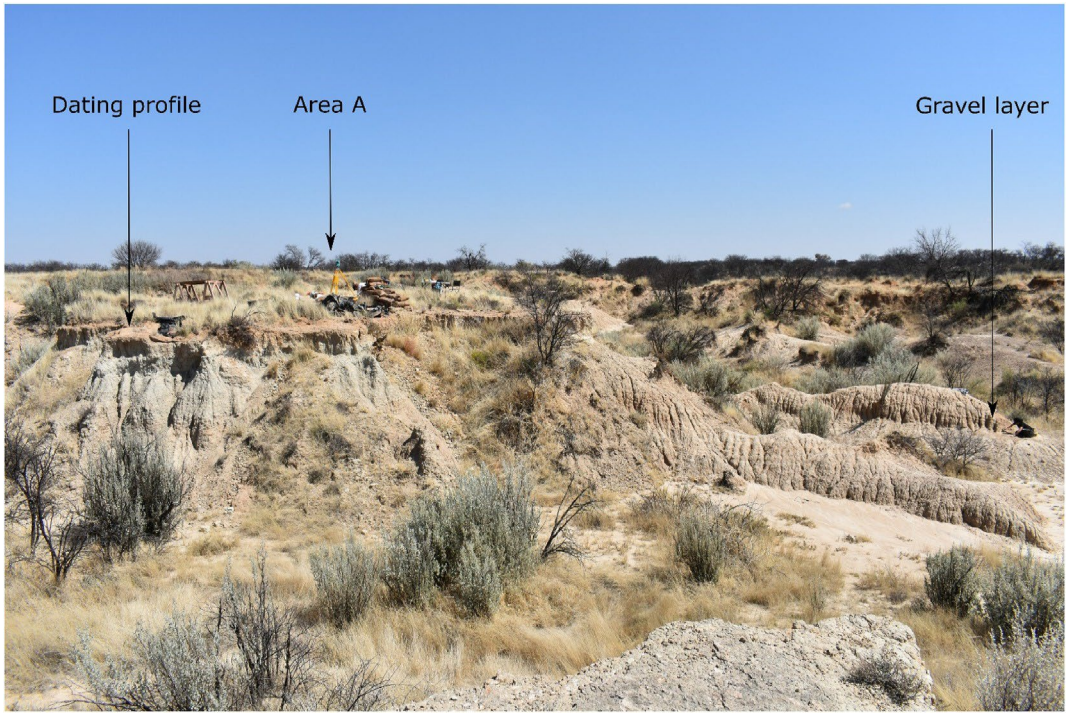

Fig. 4. View of Area A looking west, taken from Area B. Note the difference in elevation between the top of the excavation area and the bottom of the donga. The gravel layer, rich in faunal remains, is located to the north of Area A and dips underneath this area, pinching out before reaching the dating profile. The dating profile is located on the south side of Area A (visible in Fig. 5).

artifacts.

The sediments were described in the field according to color, texture, inclusions, and visible pedofeatures and categorized as Zones 1e10, beginning at the base of the dating profile in Area A (Table 1). The definition of a zone is "any regular or irregular layer of earth materials characterized as distinct from surrounding parts by some particular property or content", including sedimentologic and pedogenic differences (Gary et al., 1972: 80). In combination with further laboratory analyses, the interpretation of the different zones resulted in the characterization of sedimentary units (SUs) based on the depositional context of the sediments and any post- depositional alteration (i.e., cementation, weathering, or pedo- genesis, Fig. 5, SUs 1e7 from bottom to top). All finds were plotted using a total station (Sokkia SET 630R), including artifacts and faunal remains found in surface scatters around Areas A, B, and C. Artifacts and faunal remains were transported to the Florisbad Research Station of the National Museum Bloemfontein, where they are being studied and permanently curated.

2.2. Sampling strategy

Twenty-five bulk sediment samples for phytolith analysis and infrared spectroscopy were collected in small plastic vials at ver- tical intervals of ~10 cm from the dating profile, as well as from the excavated trenches in Area A. Twelve intact blocks of sediment for micromorphological analysis were carved from sections and jac- keted with plaster bandages for transport. The micromorphological sampling program focused on the transitions between the sedi- ment zones identified in the field and any features visible with the naked eye. Additional bulk samples were collected for lumines- cence dating from the dating profile, one of the excavated trenches, and the preserved Holocene sediments (n ¼ 7). All sediment sam-
ples were plotted using the total station (Fig. 5).

2.3. Micromorphology of sediments

After removal and consolidation, the micromorphological blocks were shipped to the Institute for Archaeological Sciences, Univer-
sity of Tübingen, Germany. Once documented and photographed, the samples were dried in an oven at ~40 °C for one week. The blocks were then embedded with a mixture of polyester resin and
styrene (7:3), catalyzed with MEKP, and left to solidify under a fume hood. They were subsequently heated to ensure the blocks were fully hardened. Solid blocks were sliced into 2-3 cm-thick slabs
with a large rock saw and then further cut down into ~6 x 8 cm chips with a tile saw. The chips were sent to Quality Thin Sections
(Tucson, Arizona, USA) where they were mounted on glass slides and polished to a thickness of 30 mm. The thin sections were scanned with a high-resolution slide scanner following the pro- cedures described by Haaland et al. (2019) with both plane- polarized light (PPL) and cross-polarized light (XPL). The slides were then analyzed using these scans, a stereomicroscope, and a petrographic microscope with magnification up to 400x and using
both PPL and XPL to characterize the sedimentary composition. The description of the sediment is based on established protocols (Macphail and Goldberg, 2017; Stoops, 2021; Stoops et al., 2018).

2.4. Fourier transform infrared spectroscopy (FTIR)

Sediments were analyzed with FTIR to determine their composition. Each sample was sieved prior to analysis to target the fraction smaller than 50 mm and thus reduce the contribution of quartz sand, which is the main component of the Lovedale sedi- ments and 'masks' the absorption bands of clay minerals (Toffolo et al., 2017). Samples were placed in contact with a diamond tip and infrared spectra were collected in attenuated total reflectance (ATR) mode in 32 scans within the 4000-400 cm^{-1} spectral range
using an Agilent Cary 630 spectrometer operated via the Agilent

Table 1
Description of zones (based on original field descriptions) and sedimentary units (based on the combination of macroscopic sediment descriptions and micromorphological analysis), ordered from top to bottom. The units and zones are numbered beginning at the base of the dating profile and moving upwards.

SU	Zones	Description
7	11	A relatively thin unit of nearly pure aeolian sand that caps SU6 in a few places. It is preserved discontinuously and varies in thickness across the site.
6	10	Preserved discontinuously across the site and only ~5 cm cap the dating profile. Dark yellowish brown, silty sand. Covered in many places with small shrubs and other plant growth, frequent root intrusions. Scattered archaeological material is present in this unit as surface finds.
5	8, 9	Pale yellow brown, very fine sandy silt. Characterized by the appearance of $CaCO_3$, large nodules/infillings/coatings in the upper part, and small nodules and few infillings in the lower part. Upper part appears somewhat bedded (Zone 2). Archaeological material is present primarily in this unit.
4	5, 6, 7	Light gray. More massive than underlying layers. Fine sandy clay. Small Fe and Mn nodules throughout but a concentration of staining and inclusions in the lower part of the unit (Zone 5).
3	4	Dark gray. Fine sandy clay with strongly prismatic peds that easily flake off the profile. Small FeeMn nodules throughout.
2	2, 3	Sharp boundary with SU1. Reddish brown. Fine sandy silt. Inclusions of Fe and Mn nodules (1 mme2 cm), Fe staining, and Fe rhizoliths increase towards top of unit.
1	1	Pale brown. Massive, silty sand. Clear burrows/channels both vertically throughout filled with sediment from SU2.

MicroLab software. Spectra were analyzed using OMNIC 9.6 and phases were identified using the infrared spectra library of the Kimmel Center for Archaeological Science, Weizmann Institute of Science (http://www.weizmann.ac.il/kimmel-arch/infrared- spectra-library), and standard literature (Chukanov, 2014; Farmer, 1974; van der Marel and Beutelspacher, 1976).

Mollusk shells (n ¼ 3) and the teeth (n ¼ 5) and bones (n ¼ 6) of small- and medium-sized ungulates were analyzed using FTIR to determine the state of preservation of aragonite and carbonate hydroxyapatite, respectively. Samples were powdered in an agate mortar and pestle and about 5 mg of each were mixed with a few mg of KBr and pressed into 7-mm pellets using a hand press. Infrared spectra were collected in transmission mode in 32 scans within the 4000-400 cm^{-1} spectral range using a Bruker Alpha spectrometer operated via OPUS 7.2. Spectra were analyzed using OMNIC 9.6 and Macros Basic 8.0. The degree of atomic order of minerals was determined following the methods of Toffolo et al. (2019b) for aragonite and Asscher et al. (2011b) for carbonate hydroxyapatite.

2.5. Phytolith analysis

Phytoliths were extracted from the bulk sediment samples ac- cording to the methodology outlined by Katz et al. (2010). Approximately 50 mg of sediment were added to a 1.5 ml tube and then mixed with 50 ml of a 6M solution of hydrochloric acid. After the chemical reaction finished, 450 ml of sodium polytungstate (r ¼ 2.4 g/ml) were added, allowing the phytoliths to rise to the top of the solution and separate from the heavier sediment. The sam- ples were centrifuged at 5500 rpm for 5 min and the resulting supernatant was pipetted into clean tubes. For the analysis, 50 ml of the supernatant were placed on a glass slide and covered with a cover slip.

Phytolith concentrations were calculated by first counting the number of phytoliths present in 16 random fields of view at 200x magnification and then the number of phytoliths in a gram of sediment was extrapolated using this total and the initial weight of the sediment. The phytoliths were identified at 200x and 400x magnification and described using the conventions laid out in the International Code for Phytolith Nomenclature 2.0 (Neumann et al., 2019) and identified according to the standard literature (Mulholland and Rapp, 1992; Piperno, 2006; Stro€mberg, 2004; Twiss et al., 1969). Phytoliths were categorized into four main groups: dicotyledonous plants (leaves/stems, wood/bark), mono- cotyledonous plants (general, inflorescences), grass silica short-cell phytoliths (GSSCPs), and weathered. Additionally, other micro- remains found in the sample were counted and described, including diatoms of various types, non-pollen palynomorphs, and microcharcoal or organic matter.

Grass short cells have long been used in paleoenvironmental studies as the different types (e.g., RONDELS, LOBATES, and SADDLES) can be linked to grasses with specific photosynthetic pathways (e.g., C_3 or C_4) and that are adapted to grow in various conditions of tem- perature and humidity (Piperno, 2006; Twiss et al., 1969). To more fully investigate these patterns, a second round of phytolith anal- ysis was carried out to identify the grass short cells following the morphotype groupings and terminology described by Rossouw (2009, 2016) and based on a comparative collection specifically created for the Free State. At least 200 individual grass short cells were identified and counted for each sample when the concen- tration allowed. Six samples contained enough GSSCPs for more detailed analysis and the resulting morphotype breakdowns were compared with the more simplified version that resulted from lower concentrations of phytoliths in general and GSSCPs more specifically.

2.6. Faunal analysis

A small collection comprising 11 faunal remains was recovered from the gravel layer and rills to the north and east of Area A (Fig. 4), the rills south of Area B, and from another gravel layer 50 m to the northeast of Area A. The finds were embedded in a cemented gravel matrix, and due to constraints related to COVID-19 lockdowns identifications were undertaken on specimens with some matrix still intact using the comparative zoological collection of the Flo- risbad Quaternary Research Station as a reference. The fauna were categorized using size classes given in Brain (1974) and age classes are based on wear, following Plug (1988). Measurements (in mm) follow von den Driesch (1976).

2.7. Lithic analysis

The recovered artifacts were grouped into debitage (whole and broken flakes and blades), cores, and tools. The tools were further subdivided into edge modified flakes and blades, scrapers, adzes, hammerstones, notches, and points. Of the MSA assemblages, the projectile points are the most distinctive component and are therefore the focus of this article.

To systematically record the attributes, individual points and blades were placed on a flat surface with the dorsal side facing up and oriented so that the surviving platforms or the bases were at the proximal position (nearest the observer) and the long axis parallel with the observer's line of sight so that the tip was in the maximum distal position. Maximum measurements were made along the long axis of the artifact and at the appropriate transverse position to measure maximum width. Maximum thickness

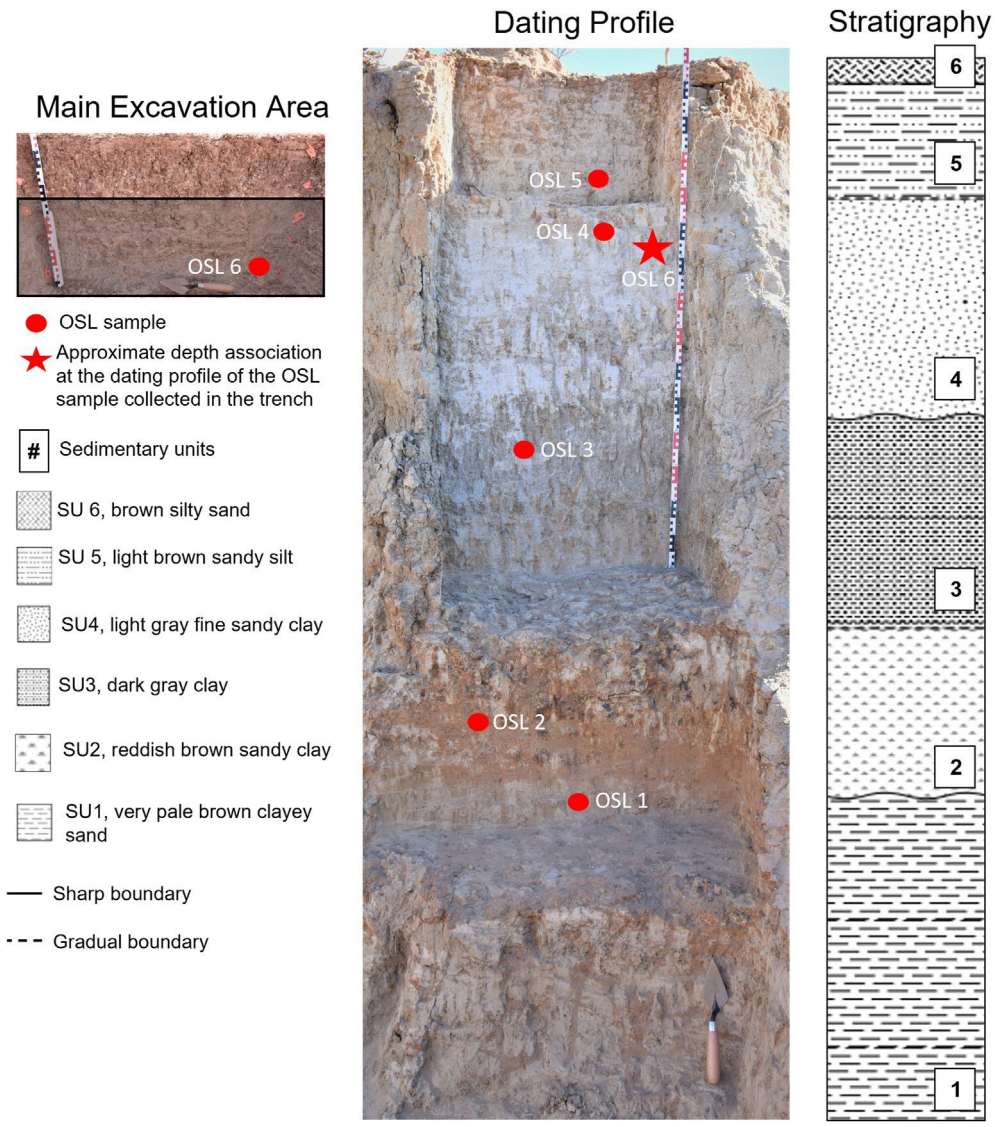

Fig. 5. Photograph of the dating profile in the center. Red circles indicate the position of the OSL samples. The red star on the photograph indicates the equivalent depth of OSL sample collected from the main excavation area, shown in the image on the far left. The dark shaded rectangle on the image of the main excavation area indicates the zone from which archaeological material was recovered. On the right is a schematic depiction of the sedimentary units present in the dating profile with their numbers indicated in the squares on the far right. (For interpretation of the references to color in this figure legend, the reader is referred to the Web version of this article.)

excluded the bulbs of percussion when present. Left and right sides were defined according to the above orientation. Broken points were either tips or bases and recorded as completely as possible. Termination definitions follow Coppe and Rots (2017).

2.8. *Optically stimulated luminescence dating (OSL)*

After cleaning the surface of the dating profile in Area A to remove sediment that was exposed to daylight (>2 cm), seven small bags of loose sediment were taken at night under subdued orange light. Three samples (LOV1, 2, and 3) were collected from the lower units, SUs 2 and 3. However, due to the highly compact and cemented nature of many of the SUs at Lovedale, sampling focused on the units related to the artifact-bearing layer, including one sample from SU5 (LOV5) and two samples from SU4 (LOV4 and 6). LOV6 was collected from the main excavation trench, about 2 m from the dating profile, immediately next to a projectile point (Fig. 5). Finally, one sample, LOV7, was collected a few meters away from the main excavation zone from the brown, alluvial sediment that is preserved discontinuously across the site (SU6).

A detailed discussion of the OSL methods can be found in Supplementary Materials 1. The equivalent doses (D_e) were measured on 100e140 mm quartz grains, applying a single-grain approach and the Single Aliquot and Regenerative dose (SAR) protocol (Murray and Wintle, 2000). Several statistical models have been proposed in the literature in order to calculate the 'mean' D_e of the distri- bution and we must distinguish models that are based on fre- quentist statistics on the one hand (the Central Age Model - CAM, Galbraith et al., 1999; the Average Dose Model - ADM, Gue›rin et al., 2017) from those based on Bayesian statistics on the other hand (Combe's et al., 2015; Philippe et al., 2019). Moreover, we must distinguish between models that assume a lognormal distribution and consider its median as the relevant D_e (the frequentist CAM and the Bayesian lognormal_Median models), those that assume a lognormal distribution and seek for the average (the frequentist ADM and the Bayesian lognormal_Average model), and those that assume a Gaussian distribution and consider its average as the relevant D_e (the Bayesian Gaussian models). All these models aside

from the lognormal_Average have been considered here.

The total dose rate is the sum of the cosmic, gamma, and beta dose rates. The alpha dose rate is considered negligible because of the HF etching treatment on the quartz grains. The cosmic dose rate was calculated using the equation of Prescott and Hutton (1994) and depends primarily on the burial depth. The gamma dose rate was measured in the field with a portable gamma spectrometer (Canberra). The beta dose rate was calculated from the U, Th, and K contents, applying the conversion factors of Gue‚rin et al. (2011), and the attenuation factors of Gue‚rin et al. (2012). Gamma and beta dose rates were corrected for attenuation by water and carbonates using the coefficients of Nathan and Mauz (2008). As it is impos- sible to know exactly when the carbonate formed, two scenarios are considered here: an early formation (mean carbonate content equal to the current one) and a late formation (mean carbonate content equal to zero).

3. Results

3.1. Formation and post-depositional processes

Local sediments are rich in quartz sand, which was removed by sieving for FTIR analysis. The fraction smaller than 50 mm is mainly comprised of clay minerals of the kaolinite and smectite groups (absorption bands at 3697, 3622e3621, 995e991, and 912- 911 cm^{-1}), and quartz (absorption bands at 797, 779, and 694 cm^{-1}) (Supplementary Materials 2). These phases are common throughout the stratigraphic sequence. In SU 5, calcite is present in small amounts in the sedimentary matrix (absorption bands at 1420 and 875 cm^{-1}), as well as calcitic nodules (Supplementary Materials 2).

Based on the in-field description and micromorphological analysis of the thin sections, seven SUs are recognized for Lovedale (Fig. 5, Table 2). Bedrock was not reached when exposing the dating

Table 2
Sedimentary units as noted in the micromorphological thin section analysis, numbered starting from the base of the sequence.

SU #	SU name	Description	Formation process
6	Brown Sand	c/f related distribution: chitonic and single spaced porphyric. Structure and voids: channels and chambers. Coarse fraction: moderately sorted. Sub-rounded, fine sand-sized quartz grains (frequent); sub-rounded, very fine and medium sand-sized quartz grains (common); sub-angular, medium/coarse silt-sized quartz grains (common); sub-angular, very fine sand-sized feldspar. Fine fraction: light brown clay. Pedofeatures: Clay coatings and infillings, FeeMn staining and nodules, earthworm channels, root channels with plant remains.	Alluvial deposition, soil formation
5	Calcrete	c/f related distribution: close porphyric. Structure and voids: channels, and chambers throughout, planar voids in the upper section. Angular blocky microstructure. Coarse fraction: Well-sorted. Sub-angular and sub-rounded, very fine to fine sand-sized quartz grains (frequent); sub-rounded, medium sand-sized quartz grains (common); sub-angular, medium to fine sand sized magnetite grains (rare), well-rounded, sand sized shale grains (rare). Fine fraction: Light yellow clay, striated and speckled b-fabric. Pedofeatures: calcium carbonate nodules (2 mme2 cm) and infillings in cracks, hypo-coatings.	Overbank deposit
4	Light Gray Clay	c/f related distribution: single spaced porphyric. Structure and voids: mostly massive with some chambers and channels. Coarse fraction: moderately sorted. Sub-rounded, fine sand-sized quartz grains (frequent); sub-rounded, very fine and medium sand-sized quartz grains (common); sub-angular, medium/coarse silt-sized quartz grains (common); sub-angular, very fine sand-sized feldspar. Fine fraction: gray clay with faint crystallitic b-fabric. Pedofeatures: infillings and coatings of the yellow birefringent clay from the upper layers, FeeMn staining and small nodules, rare calcium carbonate infillings in some voids towards the top of this unit.	Overbank deposit
3	Dark Gray Prismatic Clay	c/f related distribution: close to single spaced porphyric. Structure and voids: planar voids, chambers and channels. well-developed, highly separated, prismatic ped structure. Coarse fraction: well-sorted. Sub-angular and sub-rounded, very fine to fine sand-sized quartz grains (frequent); sub-rounded, medium sand-sized quartz grains (common); sub-angular cryptocrystalline quartz grains (rare). Fine fraction: dark gray clay with faint crystallitic b-fabric. Pedofeatures: many illuvial features, including bedded clay coatings, infillings, and intercalations, Fe and Mn nodules and staining, hypo-coatings and quasi-coatings, bioturbation in the form of small earthworm channels towards the bottom of the unit.	Alluvial, soil formation
2	Red Sandy Clay	c/f related distribution: close to single spaced porphyric. Structure and voids: chambers and some channels. Coarse fraction: moderately sorted. Sub-angular and sub-rounded, very fine to fine sand-sized quartz grains (frequent); sub-rounded, medium sand-sized quartz grains (common); sub-angular cryptocrystalline quartz grains (rare). Fine fraction: light brown/gray clay with limited speckled b-fabric. Pedofeatures: many bedded clay coatings in voids, Fe and Mn nodules, staining and impregnation, small earthworm channels.	Backwater or possible oxbow
1	Pale brown Sand	c/f related distribution: close to single spaced porphyric. Structure and voids: channels and chambers. Coarse fraction: moderately to poorly sorted. Sub-angular, medium sand-sized quartz grains (frequent); sub- angular to sub-rounded sand-sized quartz grains (common); sub-rounded, fine sand-sized quarts grains (common); sub-angular, fine sand-sized feldspar grains (few); sub-rounded, coarse sand-sized shale and dolerite grains (very few). Fine fraction: light gray clay with limited speckled b-fabric. Pedofeatures: whole and fragmented, bedded clay coatings in voids; cm-sized burrows filled with overlying sediment with a crumb structure, Fe and Mn nodules and coatings, very rare small nodules of calcium carbonate.	Low-energy alluvial deposition

profile, thus the lowest layer excavated is a lens of bedded gravels located on the opposite side of Area A and dipping towards the dating profile, from which the only *in situ* faunal remains were recovered. The latter show various degrees of preservation based on FTIR spectroscopy. The values of the full width at half maximum of the 1035 cm^{-1} peak of phosphates and splitting factor of tooth enamel from Alcelaphine teeth produced values that are consistent with the same tissue in modern bovids, indicating a good overall preservation of carbonate hydroxyapatite (Asscher et al., 2011a, 2011b). On the contrary, carbonate hydroxyapatite in the sampled bones shows signs of dissolution and recrystallization, as suggested by splitting factor values between 3.5 and 4.2. This process explains the visual appearance of some bones, which are coated by cemented gravel from the sedimentary matrix. In addition, the better-preserved bones from the gravels are composed of fluori- dated carbonate hydroxyapatite (peak at 604 cm^{-1} higher than the peak at 567 cm^{-1}) (Supplementary Materials 2). This phase, more resistant to chemical weathering, forms diagenetically when bones are exposed to groundwater rich in fluoride and it is a common occurrence in MSA faunal assemblages in the area, such as from Florisbad (Toffolo et al., 2015), or in extremely old bones (Toffolo et al., 2019a).

Shells of the freshwater bivalve *Unio caffer* were found in a point bar deposit 4 m to the north of Area A but at the same elevation as the gravel layer with vertebrate remains. FTIR showed that the shells are entirely composed of aragonite exhibiting the same de- gree of atomic order of pyrogenic aragonite (Toffolo et al., 2019b) (Supplementary Materials 2). The preservation of aragonite and the absence of secondary calcite indicate that more soluble phases, such as carbonate hydroxyapatite in bones and teeth, should be preserved at the site (Weiner, 2010). However, the fact that aragonite is poorly ordered suggests incipient recrystallization into secondary aragonite, indicating that these shells might not be suitable for stable isotopes analysis due to possible isotopic ex- change with the environment (Toffolo, 2021).

The gravel layer is stratigraphically lower compared to the lowest unit (SU1) excavated at the dating profile, which is made up of coarse, moderately sorted sand predominantly composed of quartz grains with lesser amounts of feldspars, dolerite, and shale fragments derived from the underlying bedrock (Fig. 6 A, B). This coarse fraction is similar throughout the entire sequence, differ- entiated in the other SUs primarily through size and sorting. In SU1, a small proportion of these grains have clay coatings, and both whole and discontinuous bedded clay coatings are found in the voids. Small FeeMn nodules and staining are present throughout the unit. Noted both in the field and the micromorphological analysis, SU1 shows clear evidence of bioturbation, with large, cm- sized horizontal and vertical burrows running throughout (Fig. 6 C, D). The sediment that fills these burrows has a crumb texture and clearly originates in the overlaying SU2, composed of reddish- brown fine sand. The coarse components in SU2 are nearly iden- tical to those of SU1 but the sediment is differentiated by a larger proportion of fine fraction and an increase in clay coatings and iron staining. The upper section of the red sand is characterized by a marked increase in FeeMn nodules, staining, and impregnations until FeeMn nodules become the primary component of the unit (Fig. 6 E, F). Intrusive pedofeatures such as infillings of light gray clay and bedded clay coatings in the chambers and channels occur in the middle and upper portion. Smaller burrows are present in some parts of the unit, likely from insect and earthworm activities based on the crumb-like texture of burrow infillings.

The transition between the FeeMn rich SU2 and the overlying SU3 is blurred by extensive bioturbation and thus it is unclear if this boundary is sharp or gradual. SU3 is composed of a dark gray clayey, fine sand with frequent FeeMn nodules and staining and a strongly

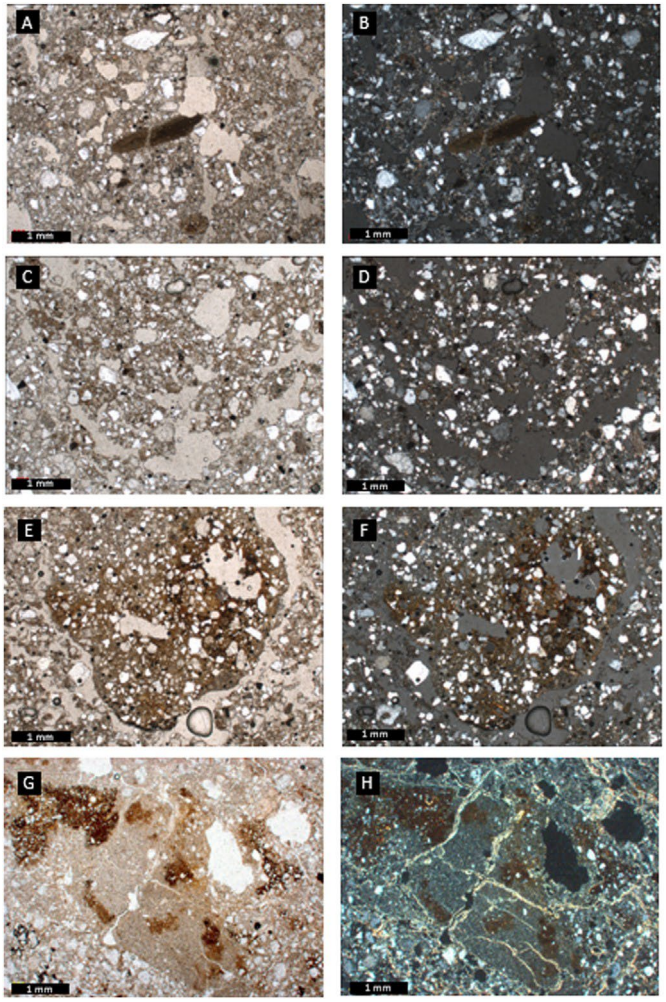

Fig. 6. Images on the left are in plane polarized light and images on the right were taken in cross polarized light. A and B show a large grain of weathered shale in SU1 from the bedrock, as well as the poorly sorted nature of the coarse fraction. C and D show the bottom of a large earthworm burrow in SU1. E and F show Fe staining and small nodules within a void in SU2. The bottom row shows large portions of the sparsely birefringent gray clay with infillings of the highly birefringent yellow clay from above, as well as areas of Fe staining in SU3. Scale bars are 1 mm. (For interpretation of the references to color in this figure legend, the reader is referred to the Web version of this article.)

prismatic ped structure. The cm-sized peds are hexagonal and flake easily from the exposed profile. There is also an increase in this unit of pedofeatures such as clay infillings, intercalations, and bedded clay coatings, most often composed of a yellow clay that appears very bright under cross-polarized light (birefringent) and which clearly contrasts with the gray, largely non-birefringent clay of the groundmass (Fig. 8 G, H). Rare, small earthworm burrows are present towards the base of the unit.

A sharp, wavy boundary marks the beginning of SU4, which is a massive light gray, fine clayey sand. The coarse fraction is similar to the underlying layers though primarily fine sand to silt. Channels are present throughout this layer, but they do not show the kind of coarse sediment infillings noted in the lower layers. However, fine clay coatings are present throughout the sample and the yellow, highly birefringent clay of these coatings contrasts with the largely non-birefringent, gray clay of the groundmass. Iron staining and small FeeMn nodules are particularly noted in the lower part of the unit and fine calcium carbonate infillings can be seen in some of the voids in the upper section. In the field, SU4 was subdivided into

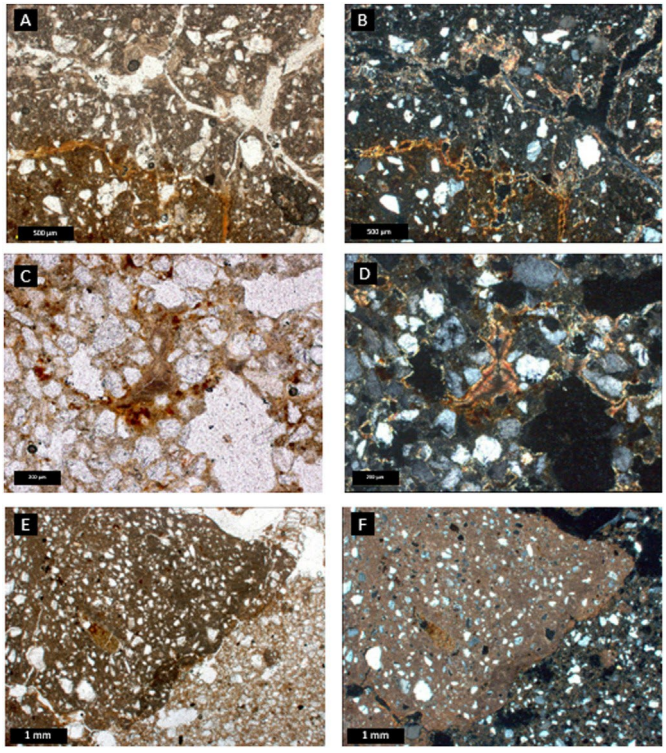

Fig. 7. Images on the left are in plane polarized light and images on the right were taken in cross polarized light. A-D show the many pedofeatures present in the lower bands of SU4, including Fe staining and nodules and bedded clay coatings around voids (A, B scale bar ¼ 500 mm; C, D scale bar ¼ 200 mm). E and F show a large, cm-sized calcite nodule at the top of SU5 (scale bar ¼ 1 mm).

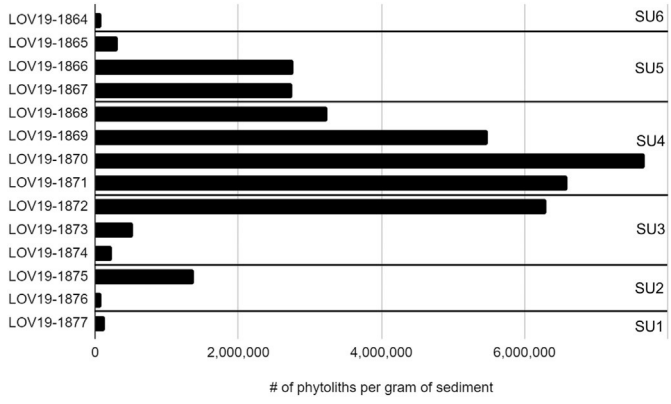

Fig. 8. Number of phytoliths per gram of sediment, horizontal lines mark the boundaries between sedimentary units.

three different zones as a band of darker sediment with Fe in- clusions was noted towards the base of the unit. The overall makeup of this zone is similar to the rest of SU4 but there is a higher concentration of illuvial features such as clay coatings within this darker zone, as well as bands of FeeMn nodules and staining near the top and bottom boundaries (Fig. 7AeD). Evidence of human occupation appears for the first time at the top of SU4.

There is a gradual boundary between SU 4 and 5. The overall sediment is similar to the rest of the underlying samples but is characterized by a coarse fraction composed of fine quartz sand and a light gray clay fine fraction. This unit is also marked by the appearance of calcium carbonate, which is first seen as filling voids in the lower part of the unit. The calcium carbonate content in- creases towards the top of the profile, including nodules (3 mme2 cm), infillings in cracks and channels, and coatings on ped faces to the point where this layer may be categorized as a weakly developed calcrete (Fig. 7 E, F). The stone artifacts are often found coated with calcium carbonate crusts and must be carefully chip- ped from the calcrete. SU5 was originally divided into two zones as the bottom of this unit is more massive while the upper portion has a weakly developed ped structure and packets of sediment are clearly separated by horizontal infillings of calcium carbonate.

The sequence is topped with a layer of strong brown, silty sand that appears to be a mix of alluvial deposits and aeolian sediment (SU6). There is a sharp boundary with SU5 and this unit is pre- served discontinuously across the site. The area of the dating profile exhibits only a few centimeters but other parts of the site feature upwards of 30 cm or more. Iron staining is common in this unit, as well as clay coatings. SU6 is often covered by small, shrubby plants and frequent root channels and other evidence for bioturbation can be seen in the thin section. SU6 is also often capped by a few centimeters of well-sorted, clearly windblown, silty sand in many parts of the site. Though not preserved at the dating profile, a unit of nearly pure aeolian sand (SU7) caps several parts of Area A.

3.2. Phytoliths

The concentration and preservation of phytoliths per gram of sediment varied throughout the profile (Fig. 8). Samples collected from both the lowest layers and the uppermost layers have low concentrations of phytoliths (<10,000 phytoliths/g) and the few phytoliths that could be identified were pitted, broken, and clearly weathered (Supplementary Fig. 5.1). This pattern contrasts with the phytolith preservation in the middle portion of the dating profile, with up to 8 million phytoliths/g in SU4 and more than two million phytoliths/g in SU5. Although a small portion of these phytoliths is weathered, the majority are well-preserved and identifiable. However, the identifiable morphotypes are primarily the most robust types (e.g., blocky, elongates, short cells) and there is only a small percentage of decorated or fragile morphotypes in the Lovedale assemblage. This pattern of preservation may indicate that at some point after their deposition the more fragile mor- photypes dissolved due to natural weathering processes (Cabanes et al., 2011). All the analyzed samples are dominated by mono- cotyledonous phytoliths, most likely from grasses though two samples did include rare sedge phytoliths (Supplementary Fig. 5.2). The phytolith assemblages in SU4 include just over 20% of phyto- liths from the wood and bark of dicotyledonous plants, whereas the majority of the other samples has 10% or less from dicots. The two upper samples have no identified dicot phytoliths. Of the mono- cotyledonous phytoliths, the assemblages are primarily composed of general morphotypes that cannot be linked to a specific plant part and only seven of the analyzed samples had phytoliths that originated in monocot inflorescences (1e3% per sample).

Grass silica short-cell phytoliths (GSSCPs) are the other main monocot component of the Lovedale samples (Fig. 9). For the upper part of SU5 and lower parts SU4, Pooid-type phytoliths dominated the assemblages, with RONDELS and RENIFORMS as the most common type as well as a smaller TRAPEZOID component. Three samples from the central part of the profile (top of SU4 and base of SU5) show a shift to Chloridoid-type phytoliths (SADDLES), with more than 50% of each sample originating in this type of grass. These SADDLES are primarily the Variant 1 type but with a small contribution of Variant 2 (Rossouw, 2009). Panicoid-type phytoliths (Variant 2 BILOBATES, POLYLOBATES) are present in all but one of the analyzed samples (5e10%).

During the phytolith analysis, other types of microremains were

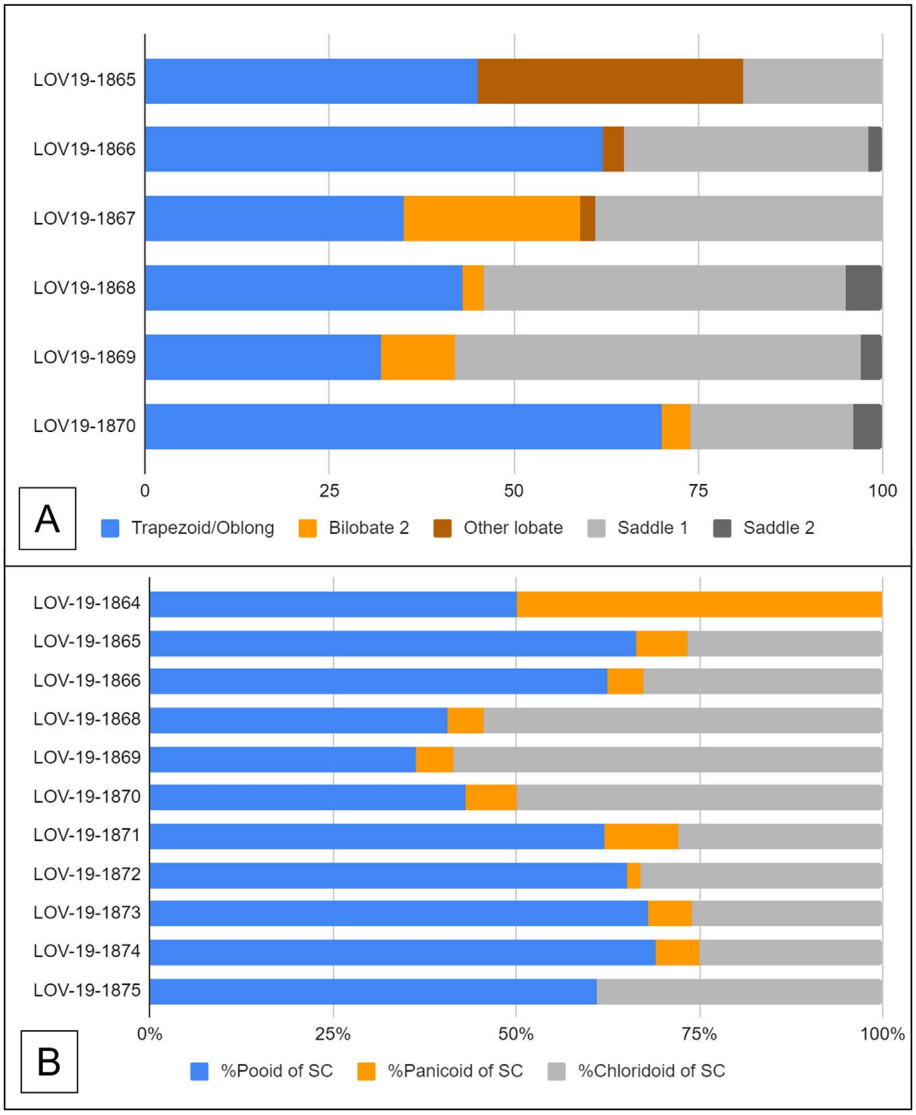

Fig. 9. A: Grass short cell breakdown by sample using more detailed analysis. 200 individual short cells were identified in each sample. B: Grass short cell breakdown by sample using simplified identifications (e.g., RONDEL, BILOBATE, SADDLE). Short cells were identified as part of the full morphotype analysis.

also counted. Diatoms and sponge spicules were noted in nearly all the samples, both common finds for areas with standing water. Non-pollen palynomorphs (NPPs) were noted in three samples from SU3.

3.3. Mammalian fauna

See Supplementary Material 3 for a full description of each of the faunal remains and attributions. Four faunal elements recov- ered from the gravel bed north of Area A may be attributed to Bovid Class IV, most likely the long-horned buffalo (*Pelorovis antiquus/ Syncerus antiquus*, Klein, 1994). Bovine material attributed to the long-horned buffalo has been documented at other MSA sites in the Free State, such as Erfkoon and Florisbad, as well as from Florisian LMA exposures on the Modder and Doring Rivers (Brink, 1987; Brink et al., 1999; Churchill et al., 2000; Rossouw, 2006).

Six additional remains are attributed to Bovid Class III, two of which could not be identified further than the size class. One mandible and vertebral body are likely identified as belonging to an Alcelaphine. Remains of Alcelaphini (*Alcelaphus*, *Connochaetes*, *Damaliscus*), have been reported from several MSA contexts in the Free State (Brink, 1987; Churchill et al., 2000; de Ruiter et al., 2011; Rossouw, 2006). A partial left mandible and a molar fragment are characterized as cf. Reduncini *Kobus leche*, a water-dependent species signifier of wetland environments (Brink, 1987).

3.4. Lithic assemblage

A total of 649 artifacts were recovered from the 2019 excavation and surface collections, 184 of which are formal tools. The assem- blage of MSA points can be divided into two groups: one that in- cludes 14 points of a unique form that we tentatively call here “Lovedale” based on the criteria described in the following sections (Fig. 10aec), and a second composed of 10 typical triangular points (Fig. 10def). The complete points are easily separated into these groups based on forms made on blades that have bifacially trimmed bases and triangular forms. The Lovedale points are a narrow tool made on a blade with trimmed tips and bifacially trimmed bases, which removes the striking platforms and most of the bulbs of percussion. The triangular points may or may not have lateral

Fig. 10. Representative specimens of Lovedale points (aec) and triangular points (def) found at Lovedale.

trimming and usually have facetted platforms. Some of these platforms fit the definition of the classic *chapeau de gendarme* platform associated with Levallois production sequences (Debe‚nath and Dibble, 2015). At a minimum, these two forms clearly indicate different production strategies.

The Lovedale points range from 53.7 mm to 138.1 mm in length, from 20.6 mm to 38.2 mm in width, and from 8.1 mm to 14.1 mm in thickness (see Fig. 10aec). The platforms have been removed on all but one, which has a small, single facetted platform that is 8.4 mm width and 6.8 mm thick. Lateral trimming varies from moderate to extensive. The bases are consistently bifacially trimmed to form a smooth, curved base and the trimming may extend the full length of the point.

The triangular points range from 45.5 mm to 114.7 mm in length, from 23.9 mm to 57.3 mm in width, and from 7.3 mm to 14.6 mm in thickness (see Fig. 10def). Most have facetted platforms although a few have dihedral platforms. The platforms vary from 15.2 mm to 40.3 mm in width and from 5.3 mm to 12.2 mm in thickness. Lateral trimming varies from none to extensive.

3.4.1. *Statistical analysis of the points*

The metric data for the points suggests there are no significant differences in lengths of triangular points and Lovedale points (Supplementary Material 4, Kruskal-Wallis H-ties ¼ 0.413, df ¼ 1, p value ¼ 0.521). The same can be said about thickness (Kruskal- Wallis H-ties ¼ 0.037, df ¼ 1, p value ¼ 0.848), but triangular points are made on a variable triangular blank with varying widths while the Lovedale points are consistently made on narrow blades (Fig. 10). This difference in widths is significant (Kurskal-Wallis H- ties ¼ 12.163, df ¼ 1, p value ¼ 0.0005). Regression plots of length and width demonstrate that the two different points have similar slopes (0.1898 mm versus 0.158 mm) but dramatically different intercepts (25.042 mm versus 14.131 mm), reflecting the significant difference in widths. There is also a great deal more variability in triangular point widths than the Lovedale point widths (see co- efficients of variation values in Supplementary Material 4 and average residuals for each length/width regression). A single Lovedale point was recovered from the site of Erfkroon, and it fits in the middle of the distribution (See Supplementary Materials 4.1). The trimmed blades from Lovedale also fit in the middle of the distribution, providing a view of the blank size of the blades used to produce Lovedale points.

Lovedale point production stages can be identified by looking at ventral trimming on both Lovedale points and trimmed blades. During the first stage, dorsal trimming shapes the curved base and ventral trimming is then used to remove the platforms and bulbs. These removals straighten the longitudinal profile created by the curved ventral surface that is accentuated by the bulb of percussion. On one trimmed blade, the ventral trimming flakes failed to remove the platform and the bulb because they terminate as step fractures and do not carry through to fully remove the platform and bulb. It appears that the production process for that artifact stopped there. On another trimmed blade, the ventral trimming removed the platform and bulb, formed the curved base, but the final tip prep- aration was not accomplished. On the Lovedale points, the distal point trimming is completed to form a final and straighter point. In sum, 1) the blades are struck, 2) initial basal trimming occurs on the dorsal sides to shape the oval base, 3) then the ventral basal trimming occurs to remove the platform and bulb, and, if that is done successfully, 4) the tip is then pointed. This set of production stages is more complex than the production process for MSA points, however no blade cores were recovered so the core preparation procedures and steps are not known.

3.4.2. *Point terminations*

Often the tips or the terminations on both forms of points are damaged. The most common terminations among both forms are feather, trimmed, and negative bend fractures. However, cone fractures and impact fractures only occur on Lovedale points. Snaps, oblique removals, rotational fragmentation, and burin scars only occur on triangular points. These data can be used to suggest that the functions and implementation-of-use differed by point form.

Table 13
Results of the equivalent dose (D_e) measurements. N: number of measured grains; n1: number of grains that pass the sensitivity and recuperation criteria; n2: number of grains that in addition, are not saturated; n3: number of grains that pass the D_0 threshold. D_0: threshold D_0 value in Gy. OD: overdispersion (%) (Galbraith et al., 1999). Four models were tested: CAM: Central Age Model; ADM: Average Dose Model, Bayesian LogNormal_M: Bayesian lognormal with calculation of the median; Bayesian Gaussian: calculation of the average.

Sample	N	n1	n2	n3	D_0	Equivalent doses (Gy)											
						CAM		OD		ADM		sigma_d		Bayesian LogNormal_M		Bayesian Gaussian	
LOV1	5200	634	301	115	120	mixture?		66	±5								
LOV2	4700	606	372	101	120	mixture?		101	±7								
LOV3	5000	670	287	96	120	144.8	±6.7	42	±3	157.4	±6.2	41	±5	150.9	±7.2	161.9	±6.9
LOV4	5000	880	353	112	120	151.7	±5.6	36	±3	160.9	±5.8	34	±3	157	±5.7	164.3	±5.5
LOV5	5900	995	398	105	120	131.4	±6.5	49	±4	147.2	±6.8	48	±5	139.4	±7.2	154.1	±6.6
LOV6	4700	983	359	84	120	159.2	±7.1	38	±3	170.2	±6.7	37	±6	167.3	±7.6	177.7	±7.1
LOV7	1200	118	100	45	50	mixture?		165	±19								

Clearly, related impact damage is more common on Lovedale points and more heavily use/pressure damage is more common on triangular points. This pattern could be related to something as simple as the points used as hafted points on either throwing or alternatively thrusting spears, or projectile point versus cutting and butchery uses.

3.5. Chronology

3.5.1. Equivalent dose (D_e)

Supplementary Fig. 1.4 displays the radial plots and D_0/D_e plots for the different samples. LOV1, LOV2, and LOV7 display high overdispersions, from 66 ± 5% to 165 ± 19% (for D_0 threshold at 120 Gy or 50 Gy, see Table 3). Macro and micromorphological ob- servations suggest that these samples are bioturbated. While we cannot precisely quantify the respective contributions to these dispersions of the beta D_e heterogeneity (due, for example, to car- bonates) and of the bioturbation, we have discarded these samples from further analyses, as they are potentially too mixed to be accurately dated. Indeed, a high degree of mixing would prevent the current estimate of the dose rates from being relevant (Gue‚rin et al., 2017).

LOV3, 4, 5, and 6 display overdispersions between 36 ± 3 and 49 ± 4%. Supplementary Fig. 1.5 presents the mean D_e versus D_0 plots following the different age models. We observe that 1) for the dose recovery measurements, the CAM gives lower D_e than the other models and the Bayesian-Gaussian models gives the higher D_e, but the discrepancy between the CAM and Gaussian models is higher than for the dose recovery ratio (e.g., Bayesian-Gauss D_e, 8e17% higher econsistent at two sigmae than the CAM De for a D_0 threshold of 120 Gy); 2) as shown by Heydari and Gue‚rin (2018), the CAM and ADM frequentist models are more sensitive to the D_0 threshold than the Bayesian models; 3) the D_e plateau that is ex- pected in the zone where no more grains are rejected because of saturation (D_0 > 120 Gy) is not clearly obtained: the D_e, whatever the model, slightly decreases when the D_0 threshold increases. It is not clear whether this is a statistical issue or a physical one. The dose recovery test does not suggest that the SAR protocol is less efficient for high D_0 values (>200Gy) than for those in the range 120e200 Gy. A single aliquot regenerative and additive dose pro- tocol (SARA, Mejdahl and Bøtter-Jensen, 1994) was attempted on LOV6 in order to assess whether or not unrecorded sensitivity change between natural and natural test dose was biasing the measurements, but this was not conclusive. On one hand, less confidence should be given to the highest D_0 threshold values because of the lower number of grains considered in the distribu- tion, but on the other hand, a slight overestimate of Ln/Tn compared to the regenerative growth curve could lead to signifi- cant (though imprecise) overestimate of the D_e when close to the saturation value (i.e., with lower D_0 values). We have fixed the D_0 threshold at 120 Gy for the final D_e and age calculations.

3.5.2. Dose rate

Table 4 displays the results for the dose rates. The cosmic dose rates stand between 0.18 ± 0.02 and 0.24 ± 0.02 Gy/ka and contribute about 10% of the total dose rates. The gamma dose rate calculated from *in situ* measurements for all samples except LOV4 stands between 0.68 ± 0.06 Gy/ka and 0.89 ± 0.09 Gy/ka. They are consistent with the gamma dose rates calculated from the U, Th, and K content (see below). This observation suggests that we can confidently use the gamma dose rate calculated from the radio- isotopic content for LOV4 (0.83 ± 0.08 Gy/ka), for which no *in situ* measurement could be performed.

The U, Th, and K contents are displayed in Supplementary Table 1.2. Current disequilibrium in the U chain is low (in most cases lack of activity for ^{226}Ra is <20% compared to the top and middle of the chain). Considering the overall ca. 30% of U contri- bution to the total dose rate, we assume that this small disequi- librium, regardless of its cause and evolution, had a negligible impact on the past mean dose rate. The beta dose rates corrected for past mean water content and current carbonate content using the early uptake carbonate hypothesis stand between 1.09 ± 0.12 Gy/ka and 1.42 ± 0.16 Gy/ka, contributing about 55% of the total dose rates. Using the late carbonate formation hypothesis, the gamma and beta dose rates are up to 6% lower though statis- tically consistent with the early uptake values. Consequently, the mean of the early and late uptake dose rates is used for the final age estimates.

3.5.3. Ages

Aside from the assumptions made regarding the dose rate cal- culations, we face two issues when calculating final ages: the lack of clear plateau in the D_e/D_0 plots that makes the final D_e and ages dependent on the D_0 threshold, as discussed above, and the dis- crepancies between the different statistical models for the calcu- lation of the relevant "mean" dose.

The systematic trend observed here (see comments in section 3.5.1, Table 5 and Fig. 11) has also been observed in other series of samples (e.g., Chevrier et al., 2020; Tribolo et al., 2022). Some au- thors (Gue‚rin et al., 2017; Heydari and Gue‚rin, 2018) have sug- gested that the CAM model and Bayesian-logNormal_Median models tend to underestimate the ages when the De are high and have argued that the ADM and Bayesian-Gaussian models would be more accurate. However, there is currently no consensus about this issue. The dose recovery experiment carried out on the Lovedale samples is of little help regarding this decision as it does not fully reflect the measurements and analyses of the burial doses and we lack other clear-cut evidence. Consequently, we have considered

Table 4
Dose rate data. The moisture and carbonate contents are calculated respectively as the mass of water or carbonate over the mass of dry non-carbonated material. They correspond to the current contents. However, for the dose rate calculation a past mean water content of 15 ± 5% has been considered (see text). With the "early uptake" hypothesis, we assume that the past mean carbonate content was similar to the present one; with the "late uptake" hypothesis, we assume that the past mean carbonate content was null. The final total dose rate is the mean of the values obtained following these two hypotheses.

			Dose rates (Gy/ka)															
			Cosmic		Early uptake of carbonates						Late uptake of carbonates						Final total	
Sample	Moisture content	Carbonate Content			Beta		Gamma		Total		Beta		Gamma		Total			
LOV1	3%	4%	0.17	±0.02	1.18	±0.13	0.69	±0.06	2.04	±0.15	1.22	±0.14	0.69	±0.06	2.08	±0.16	2.06	±0.17
LOV2	5%	8%	0.18	±0.02	1.13	±0.13	0.72	±0.06	2.03	±0.14	1.21	±0.14	0.71	±0.07	2.1	±0.16	2.06	±0.18
LOV3	7%	6%	0.19	±0.02	1.42	±0.16	0.89	±0.09	2.5	±0.18	1.49	±0.17	0.88	±0.09	2.57	±0.2	2.53	±0.22
LOV4	5%	8%	0.21	±0.02	1.27	±0.14	0.83	±0.08	2.31	±0.16	1.36	±0.16	0.88	±0.08	2.46	±0.18	2.38	±0.24
LOV5	6%	4%	0.22	±0.02	1.29	±0.15	0.84	±0.08	2.34	±0.17	1.33	±0.16	0.84	±0.08	2.38	±0.18	2.36	±0.19
LOV6	3%	3%	0.22	±0.02	1.25	±0.14	0.82	±0.07	2.3	±0.16	1.28	±0.15	0.82	±0.08	2.32	±0.17	2.31	±0.18
LOV7	3%	3%	0.24	±0.02	1.09	±0.12	0.68	±0.06	2.01	±0.14	1.11	±0.13	0.67	±0.06	2.02	±0.14	2.02	±0.15

Table 5
OSL ages for samples LOV3, 4, 5, and 6 following different statistical models. They are displayed according to the stratigraphic order.

Sample	Ages (ka)							
	CAM		ADM		Bayesian LogNormal_M		Bayesian Gaussian	
LOV5	56	±6	62	±6	59	±6	65	±7
LOV4	64	±7	67	±8	66	±8	69	±8
LOV6	69	±7	74	±7	72	±7	77	±7
LOV3	57	±6	62	±6	60	±6	64	±7

each of these models for the Lovedale dates and refer more generally to date ranges. The age of the human occupation at Lovedale thus ranges between 77 ± 7 and 56 ± 6 ka (Table 5), with a context with a Lovedale point dated to the range 77 ± 7 to 69 ± 7 ka (LOV6). However, these issues have no significant impact on the general conclusions as all the ages, regardless of the model, consistently fall within MIS 4 or late MIS 5a. A small but significant stratigraphic reversal is observed for LOV3 in SU3 and LOV6 in SU4. The reason for this reversal is unclear but may be related to rapid deposition of sediment as well as soil formation processes.

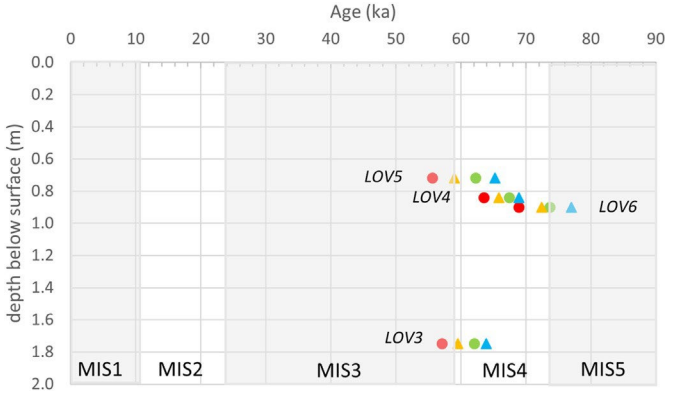

Fig. 11. OSL ages for samples LOV3, 4, 5, and 6 following different statistical models. Red circles: Central Age Model. Green circles: Average Dose Model. Yellow triangles: Bayesian LogNormal_Median model. Blue triangles: Bayesian Gaussian Model. Un- certainties are not shown for sake of clarity (the same plot including uncertainties can be found in Supplementary Fig. 1.6). (For interpretation of the references to color in this figure legend, the reader is referred to the Web version of this article.)

4. Discussion

4.1. Evolution of the river terrace and the paleoecological context of human occupation

The Pleistocene stratigraphy of Lovedale can be separated into three primary sections: the base of the sequence deposited through high-to-low energy fluvial action and post-depositionally altered through bioturbation (SU1 and 2), the middle portion with evi- dence for soil formation and an erosional hiatus (SU3), and the upper part of the profile that is characterized by another sedi- mentary gap and the formation of an incipient calcrete (SU4 and 5). Based on the fluvial sediments at the base of the profile (SU1) and the gravel deposits located to the north, it is clear that the course of the Modder River would have flowed directly through Area A. Movement towards its current position can be traced by following the point-bar deposits composed of gravel and vertebrate fauna, and the shelly sand that crops out throughout the donga between Area A and the current river channel. The fact that bones and teeth were found at the bottom of the stratigraphic sequence, and the absence of secondary phosphate nodules in SU4 and below, do not support the hypothesis that bones were present in the younger artifact layer but later dissolved due to diagenetic processes. This interpretation is consistent with the alkaline nature of the sedi- mentary matrix of the artifact-bearing layer, which promotes the preservation of carbonate hydroxyapatite (Berna et al., 2004). However, we cannot exclude complete dissolution of all secondary phosphate. Given the large surface extent of the occupation, we conclude that bones might not have been deposited in the units that were excavated. Bones were recovered *in situ* in depositional contexts of similar age and sedimentary matrix at Erfkroon, 10 km downstream (Bousman et al., in press).

As the course of the river changed, the area became first a marshy backwater, rich in plants and organic matter as indicated by the unit composed almost entirely of redoximorphic features and altered heavily through bioturbation (SU2). It is well known that the decomposition of organics can mobilize Fe and Mn, which subsequently oxidize yielding the characteristic bright red color (Vepraskas et al., 2018). This area may have continued to dry slightly as the river shifted towards its current position and remained a stable land surface for some time as a soil began to form (e.g., illuvial features, clay coatings found in SU3). This stable sur- face was followed by a period of erosion and rapid sediment deposition as large packets of massive, fine-grained sediment accumulated (SU4), leaving a wavy erosional boundary between these two units. Within SU4, there is also at least one period of a stable land surface and exposure, leading to a band of Fe nodules and illuvial features that may indicate the start of soil formation. After a possible erosional event that removed any A horizon, this zone was buried with similar massive, fine-grained material.

It is in SU4 and SU5 that the primary concentrations of phyto- liths are found. It is likely that the high degree of post-depositional alteration and bioturbation that occurred in the lowest units also

affected phytolith preservation, leading to low concentrations of highly weathered, unidentifiable phytoliths. During the periods with more stable conditions, the phytoliths were better preserved and the high concentrations allow for some interpretations of the possible environmental conditions. As mentioned above, GSSCPs are linked to grasses that follow distinct photosynthetic pathways such as C_3 and C_4 grasses. In some parts of the world these groups are correlated with arid or more humid conditions, but the situation in South Africa is complicated by regions of summer rainfall vs. winter rainfall vs. year-round rainfall and widely varying temper- atures (Ellis et al., 1980). Previous research indicates, however, that C_3 grasses are associated with the cooler, drier to mesic regions with winter rainfall whereas C_4 grasses are commonly found in areas of summer rainfall with elevated temperatures during the growing season (e.g., Cordova, 2013). C_4 grasses can also be subdivided into three subtypes: those associated with areas of high summer rainfall (NADP-me), those correlated with more arid areas and low summer rainfall (NAD-me), and those grasses that grow in areas of either intermediate rainfall or areas that stay continually moist in a region with otherwise low summer rainfall conditions (PCK) (Russell-Gibbs et al., 1990; Schulze et al., 1996; Vogel et al., 1978). Previous research indicates that proportions of various grass short cell types can be linked to each of these photosynthetic pathway types and subtypes (Rossouw, 2009, 2016). C_3 grasses are linked to the trapeziform morphotype group that includes TRAPE- ZOIDS, RONDELS, OBLONGS, and RENIFORMS, whereas C_4 grasses are associ- ated with two variants of the SADDLE morphotype. The NADP-me type is primarily linked to the LOBATE classes and the NAD-me and PCK types are correlated with the SADDLE morphotypes.

The lower part of SU4 is characterized by phytoliths associated with Pooid, C_3 grasses that are adapted to cooler growing seasons. A shift to Chloridoid type grasses that produced higher concentra- tions of SADDLE phytoliths can be seen in the upper part of SU4 and the base of SU5. These types of grasses tend to flourish under warmer growing conditions. A combination of primarily Variant 1 and 2 SADDLE morphotypes with a small percentage of Variant 2 BILOBATES was found in these samples and previous research has linked this kind of mix to the NAD-me subtype of C_4 grasses, which tend to be found in areas that are warmer, more arid, and see less summer rainfall (Rossouw, 2016). The upper part of the profile again returns to the C_3 type grasses and then poor preservation and limited identification at the very top.

The shift to C_4, possibly more arid type vegetation also coincides with increasing amounts of calcium carbonate coatings in thin section, calcite nodules in the sediment, and calcrete formation, as well as the first appearance of archaeological material (top of SU4). The occurrence of stone tools indicates the development of a stable land surface near the river. The fact that artifacts were concentrated within 20 cm thickness lends support to the interpretation that they were found *in situ* or minimally displaced by the subsequent deposition of fine-grained alluvium, which provided the substrate for the present-day topsoil (SU6).

The Lovedale sequence can be compared with the Orangia terrace at Erfkroon, 10 km downstream, where the Lower Grey Bed produced OSL dates at ~85 ka in its middle portion and ~55 ka toward the top, thus overlapping with Lovedale and confirming low-energy river deposition during MIS 5a and 4 (Bousman et al., in press). The two sequences share a similar sedimentary matrix rich in gray clay and the presence of preserved B horizons characterized by prismatic structure, although the Lower Gray Bed at Erfkroon is much richer in calcite nodules and does not feature extensively oxidized zones consistent with marshy environments (Bousman et al., in press; Morris, 2019). Phytolith assemblages dated to ~60 ka, slightly younger than the assemblages presented here, are characterized by a mixture of C_3 and C_4 morphotypes (the latter including Chloridoideae and Panicoideae) that show the complex interplay between temperatures and precipitation regime in the summer rainfall zone (Bousman et al., in press).

4.2. Late Pleistocene paleoenvironments in the interior plateau of South Africa

The results presented herein allow a first glimpse of the paleo- ecology of the Free State grasslands at the onset of MIS 4. In the following sections we present the archaeological and environ- mental context of MIS 5a and 4 in the interior plateau of South Africa, and the place of Lovedale within it.

4.2.1. MIS 5a

On the coast of South Africa and adjacent lowlands, MIS 5a (~83e71 ka; Lisiecki and Raymo, 2005) is characterized by wetter and warmer climatic conditions, concurrently with the develop- ment of the SB cultural tradition, which is documented at several cave sites (Chase, 2010; Hahn et al., 2021; Henshilwood, 2012; Scott and Neumann, 2018). However, at Witpan (Northern Cape), close to the Namibian border, Kalahari dune activity indicative of dry con- ditions is dated to ~77e76 ka (Telfer and Thomas, 2007), and Namibian speleothems cease growing between ~83e77 ka (Robbins et al., 2016). The palynological record at Tswaing crater (Gauteng), in the northern interior, indicates the presence of savanna woodland between ~75e73 ka, and cooler conditions after ~73 ka (Scott, 2016; Scott and Neumann, 2018), which are consis- tent with data from the south coast (d'Errico et al., 2017).

The sites in the interior plateau featuring MIS 5a deposits are the Kathu Pan complex (Northern Cape), Florisbad, Baden-Baden, Erfkroon, Lovedale, Rose Cottage Cave (Free State), and Melikane (Lesotho). At Kathu Pan, the deposition of organic-rich sediments (marsh) in KP1 Bed 7 and KP9 Bed 10 at the transition between MIS 5b and 5a (~84 ka), indicates wet conditions (Lukich et al., 2020). At Florisbad, 400 km to the southeast, nearly 2 m of green lacustrine sands (Unit 4) rich in glauconite and illite, which are clay minerals that form underwater, overly a thick beach deposit that accumulated starting from ~121 ka, although the age of the green sands is not constrained by multiple measurements (Grün et al., 1996; Toffolo et al., 2017). Unfortunately, this sedimentary unit did not produce pollen and thus we lack information about the associated plant cover (Scott et al., 2019). At the Baden-Baden spring site, 30 km north of Florisbad, greenish-gray sandy clay dated to ~77 ka is interpreted as evidence of increased spring flow caused by wetter conditions (van Aardt et al., 2016). At Erfkroon, 45 km southwest of Florisbad, multiple MSA occupations have been dated between ~99 and ~55 ka in the low-energy alluvial Lower Gray Bed within the Modder River Orangia Terrace (Bousman et al., in press; Brink et al., 2016). Results from Erfkroon are consistent with the overbank deposits that we observed in the Lovedale dating profile. In addi- tion, the Florisian fauna and the phytolith assemblages dominated by C_3 grasses below SU4 are indicative of a well-watered environ- ment. Further to the east, at Rose Cottage Cave, charcoal assem- blages from the latest MIS 5 occupation at ~78 ka (layer Kusel, pre-HP) show the presence of deciduous woodland typical of a humid environment (Lennox and Wadley, 2022; Pienaar et al., 2008). In the Maloti-Drakensberg, the basal portion of the Melikane sequence (Layers 30e27), which includes pre-HP artifacts dated to ~83e80 ka, yielded a phytolith assemblage dominated by C_3 grass short cells, consistent with a humid and cool grassland at high altitude (Pazan et al., 2022; Stewart et al., 2012, 2016).

Therefore, despite the small amount of available data, it appears that at least some portions of the Northern Cape, Free State, and Lesotho experienced localized wet conditions at the end of MIS 5, and are thus in agreement with evidence from the coast (Lukich

and Ecker, 2022). This does not come entirely as a surprise, if we consider faunal remains. The Florisian LMA, which spans the range ~600-10 ka, is characterized by a number of water-dependent mammal species that are currently extinct in the interior of South Africa but survive in wetlands to the north. One of these, *K. leche*, has been found in Middle Pleistocene deposits at Florisbad, Vlakkraal, and Kathu Pan (Brink, 1987; Brink and Henderson, 2001; Mohale et al., 2022; Wells et al., 1942), as well as the Vet River (de Ruiter et al., 2011). The *K. leche* mandible found in the gravel layer at Lovedale confirms the wetland character of the site. In addition, a related species, *K. ellipsiprymnus* (waterbuck), has been recovered at Florisbad and Erfkroon, as well as *Hippopotamus amphibius* (hippopotamus) (Brink, 1987; Brink and Henderson, 2001; Churchill et al., 2000). The small grazer *Antidorcas bondi* (Bond's springbok), another key extinct species of the Florisian LMA, has been found in Middle and Late Pleistocene deposits at Florisbad, Vlakkraal, Erfkroon, and Rose Cottage Cave (Brink and Lee-Thorp, 1992; Ecker and Lee-Thorp, 2018). Based on faunal assemblages, these sites are thought to be part of a network of Florisian wetlands associated with paleolakes and rivers that encompassed the South African interior and extended into northern Botswana at various stages during the Middle and Late Pleistocene, in spite of the general trend towards greater aridity observed along the coast during MIS 4 (Brink, 2016). This resource-rich environment thus had the potential to support humans during periods of prolonged climatic stress.

4.2.2. MIS 4

With the transition to the MIS 4 stadial (~71e57 ka; Lisiecki and Raymo, 2005), the south coast becomes drier and colder (Woillez et al., 2014), conditions that might have influenced the develop- ment of the HP cultural tradition (d'Errico et al., 2017). On the contrary, the east coast is more humid between ~68e63 ka (Hahn et al., 2021; Scott and Neumann, 2018). In the northern interior, the Tswaing pollen record indicates the presence of warm, dry grassy savanna at ~63e62 ka and drought conditions, supporting evidence from Indian Ocean cores (Chase, 2021; Partridge et al., 1998; Scott, 2016). Only a few sites in the interior plateau include MIS 4 deposits. Kathu Pan 6 (Bed 9, ~74 ka, HP) and 9 (Bed 9, older than ~55 ka) are characterized by the accumulation of aeolian sand and the absence of organic-rich marshy sediments during MIS 4, indicating drier conditions compared to MIS 5a (Lukich et al., 2020; Lukich and Ecker, 2022). As previously noted, after MIS 5e Florisbad was covered by a poorly dated lake transgression (Unit 4), whereas the Modder River deposited the Lower Gray Bed sediments at Erfkroon until the end of MIS 4 (Bousman et al., in press; Lyons et al., 2014; Toffolo et al., 2017). At Erfkroon, the excavation and dating of articulated carcasses of *Equus capensis* and *Megalotragus priscus*, and the discovery of other articulated skeletons in the same stratigraphic position, suggest that between 62.5 and 60.9 ka there was a significant drought, extreme enough to cause widespread starvation of herbivores in the Modder River basin (Bousman et al., in press). Deciduous woodland vegetation persisted around Rose Cottage Cave, based on charcoal assemblages from layers Engela to Suzy (HP), dated to ~65e60 ka (Lennox and Wadley, 2022). This scenario is consistent with the phytolith assemblages recovered at the open-air site Sunnyside 1 (eastern Free State), Unit 7, dated to ~63 ka, which are rich in C_3 grasses and non-grass aquatic herbs (Henderson et al., 2006; Kent and Scholtz, 2003). At Melikane, Layers 26e22 yielded an HP artifact assemblage, dated to ~61 ka at the top of this portion of the stratigraphic sequence. The phytolith assemblage is still dominated by C_3 grasses, although the C_4 component increased by 30% compared to MIS 5a and mainly with regard to Panicoideae. This has been interpreted as indicative of slightly warmer temperatures or lowered pCO_2 levels (Stewart et al., 2012, 2016). Evidence from these few sites lends support to a trend towards drier conditions during late MIS 4 in the central interior, although data is too scarce to draw definitive conclusions. At Lovedale, sediment deposition by the Modder River at the end of MIS 5a set the stage for human occupation at some point between ~77 and ~69 ka and continued throughout MIS 4 (Table 5). The transition between MIS 5a-4 at Lovedale was a period char- acterized by a relatively drier climate compared to contemporary sites to the east, such as Rose Cottage Cave and Melikane, based on the large Chloridoideae component in the phytolith assemblages. This seems to reflect increased aridity in the open grasslands of the western Free State, as opposed to the more temperate conditions at the foot and top of the Maloti-Drakensberg, and in accordance with results from Kathu Pan in the Kalahari Basin. However, the variety of environmental proxies employed at the different sites taken into consideration hinders direct comparisons. Alluvial deposition at Lovedale and Erfkroon during MIS 5a and 4 depends on long-term climate patterns at the regional scale. Phytolith assemblages, instead, are more sensitive to short-term changes in local rainfall rates, such as the peak in aridity observed at Lovedale in early MIS 4, and the overall temperate conditions until the end of MIS 4. Similar terrestrial records, as well as stable isotopes from tooth enamel and plant lipid biomarkers, are required from a greater number of interior sites in order to better understand Late Pleistocene environmental change.

At present, Lovedale is the only open-air occupation in the central interior plateau of South Africa dated to late MIS 5a-early MIS 4. It is noteworthy that the only MSA presence in this stretch of the Modder occurred at a time of local dry conditions. The stable land surfaces of SU4 and 5 offered a preparation area for human groups hunting along the course of the river, perhaps stopping at Lovedale to knap stone tools as evidenced by the lithic assemblage that includes all stages of the knapping process. The two distinct types of points mentioned above raise the issues of the function of these tools. For example, the two types may have both been pro- jectile points but with different delivery methods. Another possi- bility is the use of the triangular points as part of thrusting spears whereas the Lovedale points, which are seemingly more balanced and aerodynamic, may have been used on throwing spears that were perhaps propelled with a spear thrower. It is worth noting that the preserved MSA wooden artifact at Florisbad with a lenticular cross section and roughened end might have been the handle of a spear thrower and not a throwing stick as previously suggested (Bamford and Henderson, 2003). There is also the pos- sibility that the triangular points were not part of projectile objects but instead used for cutting as a knife and mounted on a short handle. This use may be supported by the type of pressure damage seen on some of these tools that can be caused by butchery. Much more research is needed to answer these questions, but this dis- cussion begins to address the nature of MSA tool design strategy used in the western Free State.

The point assemblages from Lovedale demonstrate that the systematic and repetitive production of narrow points with bifa- cially trimmed bases occurred in the western Free State. Similar points are present 30 km to the east at Vlakkraal (Wells et al., 1942), 75 km to the east at Kranskraal (van Hoepen, 1932), in the Vaal River at Sheppard Island (van Riet Lowe, 1931), and in the pre-HP layer LEN at Rose Cottage Cave, dated to ~96e65 ka (Harper, 1997; Pienaar et al., 2008; Valladas et al., 2005). Other possible parallels, outside the Free State, have been found at Olieboompoort Bed 2 (Mason, 1969), and Varsche Rivier 003 at the contact between AL 04 (~46 ka) and AL 05 (~55 ka) (Steele et al., 2016).

The Lovedale points appeared at a time when the SB tradition was present at several sites along the coast (Jacobs and Roberts, 2017) and the HP was well-developed at Diepkloof (Tribolo et al.,

2013) and Kathu Pan (Lukich et al., 2019). At Pinnacle Point 5e6, occupation dated to ~71 ka is dominated by a micro-blade assem- blage and lacks a clear SB occupation present at other contempo- rary sites (Brown et al., 2012). The accumulating record suggests MSA peoples practiced a complex series of technological strategies during MIS 5a and 4. No segments or other tools typical of the HP have been found at Lovedale, and the closest assemblage was recovered from layer EMC at Rose Cottage Cave, dated to ~66 ka (Pienaar et al., 2008; Soriano et al., 2007). Similarly, the closest SB assemblage was found at Sibudu, about 500 km to the east (Soriano et al., 2015), although a double-tipped, bifacially trimmed point made on hornfels was documented at Vlaakraal (Wells et al., 1942). The absence of HP and SB occupations in the western Free State begs the question of what relationship exists between these in- dustries and the Lovedale assemblage. The first issue to be addressed that would help resolve this question is one of contemporaneity between the coastal assemblages and the west- ern Free State assemblages. Resolving that question, and apparent chronological discrepancies (e.g., Lukich et al., 2019; Tribolo et al., 2013), would have important implications for the ebb and flow of human populations during this period of the Pleistocene.

5. Conclusions

At the Lovedale donga, along the Modder River in the Free State, we found evidence of human occupation dated to ~77e56 ka by OSL. The MSA lithic assemblage, which has few parallels and almost all of them in the Free State, clearly indicates that the occupation was related to hunting activities that took place close to the river. Despite the limitations posed by active sedimentary systems, we have shown how a careful micro-geoarchaeological approach can enable the reconstruction of the paleoecological context of human occupation in an open landscape and aid in the estimations of its age. Over the last ~80 ka, the Modder River provided a wetland environment consistent with the network of Florisian wetlands that punctuated the interior of southern Africa during the Middle and Late Pleistocene. These paleoenvironments supported large animal populations and thus human groups and had the potential to continue to supply these populations even during periods of climatic stress. A peak in arid conditions overlaps with human occupation at Lovedale, as shown by phytolith assemblages, and indicates that the river was a focal resource for human subsistence strategies. Sedimentary evidence seems to suggest similar condi- tions at Kathu Pan in the Kalahari Basin. However, a trend towards greater aridity in the interior of South Africa during late MIS 4 is not readily apparent, perhaps due to the different types of environ- mental proxies used at the few well-dated sites. Further research is required to understand the evolution of paleoenvironments in the grasslands of the Free State during the Late Pleistocene, and the variability in stone tool production in relation to the coast. Only by knowing the connections between different ecosystems of south- ern Africa will it be possible to piece together human dispersal throughout the subcontinent.

Author contributions

Michael Toffolo designed the research and Kristen Wroth, Chantal Tribolo, C. Britt Bousman, Liora Kolska Horwitz, Lloyd Roussow, and Michael Toffolo carried out the field work. Kristen Wroth, Michael Toffolo and Christopher Miller performed the micromorphological analysis. Kristen Wroth and Michael Toffolo performed infrared spectroscopy. Kristen Wroth performed the phytolith analysis, Chantal Tribolo performed the luminescence dating, Liora Kolska Horowitz performed the faunal analysis, and C. Britt Bousman performed the lithic analysis. All the co-authors analyzed the data, wrote the paper, and discussed and edited the manuscript based on the reviews.

Declaration of competing interest

The authors declare that they have no known competing financial interests or personal relationships that could have appeared to influence the work reported in this paper.

Acknowledgements

Fieldwork was carried out under the auspices of the Florisbad Quaternary Research Department, National Museum Bloemfontein. The excavation permit was issued to Lloyd Rossouw and Michael Toffolo by the South African Heritage Resources Agency (permit ID 2862). Research was funded by a grant from the Deutsche For- schungsgemeinschaft to Christopher Miller (grant n. MI 1748/4e1), and by the National Museum Bloemfontein. Michael Toffolo was funded by a grant from IdEx Bordeaux (grant n. ANR-10-IDEX-03- 02). Preliminary research at Lovedale was supported by a US Na- tional Science Foundation grant to C. Britt Bousman and James Brink. We would like to thank Frans Du Toit, owner of the Lovedale Farm, for granting permission to conduct fieldwork on his property and for his continued interest in the prehistory of the Free State and unwavering support of our work. We wish to thank Isaac Thapo, Jacob Maine, Abel Dichakane, Peter Mdala, Johannes Motshabi and Moses Mahloko for their assistance during fieldwork. We are grateful to Tria Oersen and Jaco Smith for facilitating our stay at the Florisbad Research Station during fieldwork seasons, to Sharon Holt for helping us sorting through collections at Florisbad, and to Cor- nie van Huyssteen for lending us a polarizing microscope during excavations. We would also like to thank Paolo Villa and Alex Mackay for generously sharing the results of their research on MSA lithic assemblages. Finally, we thank the Editor and two anonymous reviewers for their comments and suggestions, which helped improve the manuscript. This work is dedicated to the memory of the late James Simpson Brink, our friend and colleague.

Appendix A. Supplementary data

Supplementary data to this article can be found online at https://doi.org/10.1016/j.quascirev.2022.107455.

References

Acocks, J.P.H., 1975. Veld types of South Africa. Mem. Bot. Surv. S. Afr. 40, 1e128.
Asscher, Y., Regev, L., Weiner, S., Boaretto, E., 2011a. Atomic disorder in fossil tooth and bone mineral: an FTIR study using the grinding curve method. Arch- e,oSciences 35, 135e141.
Asscher, Y., Weiner, S., Boaretto, E., 2011b. Variations in atomic disorder in biogenic carbonate hydroxyapatite using the infrared spectrum grinding curve method. Adv. Funct. Mater. 21, 3308e3313.
Backwell, L., d'Errico, F., Wadley, L., 2008. Middle Stone Age bone tools from the Howiesons Poort layers, Sibudu Cave, South Africa. J. Archaeol. Sci. 35, 1566e1580.
Backwell, L., Bradfield, J., Carlson, K.J., Jashashvili, T., Wadley, L., d'Errico, F., 2018. The antiquity of bow-and-arrow technology: evidence from Middle Stone Age layers at Sibudu Cave. Antiquity 92, 289e303.
Bamford, M.K., Henderson, Z.L., 2003. A reassessment of the wooden fragment from Florisbad, South Africa. J. Archaeol. Sci. 30, 637e651.
Bar-Matthews, M., Marean, C.W., Jacobs, Z., Karkanas, P., Fisher, E.C., Herries, A.I.R., Brown, K., Williams, H.M., Bernatchez, J., Ayalon, A., Nilssen, P.J., 2010. A high resolution and continuous isotopic speleothem record of paleoclimate and paleoenvironment from 90 to 53 ka from Pinnacle Point on the south coast of South Africa. Quat. Sci. Rev. 29, 2131e2145.
Barker, C.H., 2011. Utilising published data for DTM construction and drainage basin delineation in the Modder River catchment, Free State, South Africa. S. Afr. Geogr. J. 93, 89e103.
Berna, F., Matthews, A., Weiner, S., 2004. Solubilities of bone mineral from archaeological sites: the recrystallization window. J. Archaeol. Sci. 31, 867e882. Bousman, C.B., Brink, J.S., Rossouw, L., Bateman, M.D., Morris, S.E., Meier, H., Cohen,

B., Trower, G., Herries, A.I.R., Palmison, M., Ringstaff, C., Thornton-Barnett, S., Dworkin, S., (in press). Erfkroon: late Quaternary alluvial geology, paleoenvir- onments and Stone Age archaeology in the western Free State, South Africa, in: Beyin, A., Wright, D.K., Wilkins, J., Bouzouggar, A., Olszewski, D.I. (Eds.), Handbook of Pleistocene Archaeology of Africa: Hominin Behavior, Geography, and Chronology. Springer.

Brain, C.K., 1974. Some suggested procedures in the analysis of bone accumulations from southern African Quaternary sites. Ann. Transvaal Mus. 29, 1e8.

Brink, J.S., 1987. The archaeozoology of Florisbad, Orange Free State. Mem. Nas. Mus. Bloemfontein 24, 1e151.

Brink, J.S., 1988. The taphonomy and palaeoecology of the Florisbad spring fauna. Palaeoecol. Afr. Surround. Isl. 19, 169e179.

Brink, J.S., Lee-Thorp, J.A., 1992. The feeding niche of an extinct springbok, *Anti- dorcas bondi* (Antelopini, Bovidae), and its palaeoenvironmental meaning. South Afr. J. Sci. 88, 227e229.

Brink, J.S., Berger, L.R., Churchill, S.E., 1999. Mammalian fossils from erosional gullies (dongas) in the Doring River drainage, central Free State, South Africa. In: Berger, C., Manhart, H., Peters, J., Schibler, J. (Eds.), Historia animalium ex ossibus. Festschrift Fur Angela von den Driesch zum 65 Geburtstag, pp. 79e90. Brink, J.S., Henderson, Z.L., 2001. A high-resolution Last Interglacial MSA horizon at Florisbad in the context of other open-air occurrences in the central interior of southern Africa: an interim statement. In: Conard, N.J. (Ed.), Settlement Dy- namics of the Middle Paleolithic and Middle Stone Age. Kerns Verlag, Tübingen, pp. 1e20.

Brink, J.S., 2016. Faunal evidence for a mid- and late Quaternary environmental change in southern Africa. In: Knight, J., Grab, S.W. (Eds.), Quaternary Envi- ronmental Change in Southern Africa: Physical and Human Dimensions. Cam- bridge University Press, Cambridge.

Brink, J.S., Bousman, C.B., Grün, R., 2016. A reconstruction of the skull of *Mega- lotragus priscus* (Broom, 1909), based on a find from Erfkroon, Modder River, South Africa, with notes on the chronology and biogeography of the species. Palaeoecol. Afr. 33, 71e94.

Brown, K.S., Marean, C.W., Herries, A.I.R., Jacobs, Z., Tribolo, C., Braun, D., Roberts, D.L., Meyer, M.C., Bernatchez, J., 2009. Fire as an engineering tool of early modern humans. Science 325, 859e862.

Brown, K.S., Marean, C.W., Jacobs, Z., Schoville, B.J., Oestmo, S., Fisher, E.C., Bernatchez, J., Karkanas, P., Matthews, T., 2012. An early and enduring advanced technology originating 71,000 years ago in South Africa. Nature 491, 590e593. Bruch, A.A., Sievers, C., Wadley, L., 2012. Quantification of climate and vegetation from southern African Middle Stone Age sites e an application using Late Pleistocene plant material from Sibudu, South Africa. Quat. Sci. Rev. 45, 7e17. Bruner, E., Lombard, M., 2020. The skull from Florisbad: a paleoneurological report. J. Anthropol. Sci. 98, 89e97.

Burrough, S.L., Thomas, D.S.G., Bailey, R.M., 2009a. Mega-Lake in the Kalahari: A Late Pleistocene record of the Palaeolake Makgadikgadi system. Quat. Sci. Rev. 28, 1392e1411.

Burrough, S.L., Thomas, D.S.G., Singarayer, J.S., 2009b. Late Quaternary hydrological dynamics in the Middle Kalahari: Forcing and feedbacks. Earth Sci. Rev. 96, 313e326.

Burrough, S.L., 2016. Late Quaternary environmental change and human occupation of the southern African interior. In: Jones, S.C., Stewart, B.A. (Eds.), Africa from MIS 6-2. Springer, Dordrecht, pp. 161e174.

Cabanes, D., Weiner, S., Shahack-Gross, R., 2011. Stability of phytoliths in the archaeological record: a dissolution study of modern and fossil phytoliths. J. Archaeol. Sci. 38, 2480e2490.

Carr, A.S., Chase, B.M., Mackay, A., 2016. Mid to Late Quaternary landscape and environmental dynamics in the Middle Stone Age of southern South Africa. In: Jones, S.C., Stewart, B.A. (Eds.), Africa from MIS 6-2. Springer, Dordrecht, pp. 23e48.

Chase, B.M., Meadows, M.E., 2007. Late Quaternary dynamics of southern Africa's winter rainfall zone. Earth Sci. Rev. 84, 103e138.

Chase, B.M., 2010. South African palaeoenvironments during marine oxygen isotope stage 4: a context for the Howiesons Poort and Still Bay industries. J. Archaeol. Sci. 37, 1359e1366.

Chase, B.M., 2021. Orbital forcing in southern Africa: towards a conceptual model for predicting deep time environmental change from an incomplete proxy re- cord. Quat. Sci. Rev. 265, 107050.

Chazan, M., Berna, F., Brink, J., Ecker, M., Holt, S., Porat, N., Lee-Thorp, J., Horwitz, L.K., 2020. Archeology, environment, and chronology of the Early Middle Stone Age component of Wonderwerk Cave. J. Paleol. Archaeol. 3, 302e335.

Chevrier, B., Lespez, L., Lebrun, B., Garnier, A., Tribolo, C., Rasse, M., Gue,rin, G., Mercier, N., Camara, A., Ndiaye, M., Huysecom, E., 2020. New data on settlement and environment at the Pleistocene/Holocene boundary in Sudano-Sahelian west Africa: interdisciplinary investigation at Fatandi V, eastern Senegal. PLoS One 15, e0243129.

Chukanov, N.V., 2014. Infrared Spectra of Mineral Species. Springer.

Churchill, S.E., Brink, J.S., Berger, L.R., Hutchinson, R.A., Rossouw, L., Stynder, D., Hancox, P.J., Brandt, D., Woodborne, S., Loock, J.C., Scott, L., Ungar, P., 2000. Erfkroon: a new Florisian fossil locality from fluvial contexts in the western Free State, South Africa. South Afr. J. Sci. 96, 161e163.

Clark, J.L., Kandel, A.W., 2013. The evolutionary implications of variation in human hunting strategies and diet breadth during the Middle Stone Age of southern Africa. Curr. Anthropol. 54, S269eS287.

Clarke, R.J., 1985. A new reconstruction of the Florisbad cranium, with notes on the site. In: Delson, E. (Ed.), Ancestors: the Hard Evidence. Alan R. Liss, New York, pp. 301e305.

Codron, D., Brink, J.S., Rossouw, L., Clauss, M., 2008. The evolution of ecological specialization in southern African ungulates: competition- or physical envi- ronmental turnover? Oikos 117, 344e353.

Combe's, B., Philippe, A., Lanos, P., Mercier, N., Tribolo, C., Guerin, G., Guibert, P., Lahaye, C., 2015. A Bayesian central equivalent dose model for optically stim- ulated luminescence dating. Quat. Geochronol. 28, 62e70.

Coppe, J., Rots, V., 2017. Focus on the target. The importance of a transparent fracture terminology for understanding projectile points and projecting modes. J. Archaeol. Sci.: Report 12, 109e123.

Cordova, C.E., 2013. C3 Poaceae and Restionaceae phytoliths as potential proxies for reconstructing winter rainfall in South Africa. Quat. Int. 287, 121e140.

d'Errico, F., Henshilwood, C., Vanhaeren, M., van Niekerk, K., 2005. *Nassarius kraussianus* shell beads from Blombos Cave: evidence for symbolic behaviour in the Middle Stone Age. J. Hum. Evol. 48, 3e24.

d'Errico, F., Henshilwood, C.S., 2007. Additional evidence for bone technology in the southern African Middle Stone Age. J. Hum. Evol. 52, 142e163.

d'Errico, F., Backwell, L.R., Wadley, L., 2012. Identifying regional variability in Middle Stone Age bone technology: the case of Sibudu Cave. J. Archaeol. Sci. 39, 2479e2495.

d'Errico, F., Banks, W.E., Warren, D.L., Sgubin, G., van Niekerk, K., Henshilwood, C., Daniau, A.-L., Sa›nchez Gon~i, M.F., 2017. Identifying early modern human ecological niche expansions and associated cultural dynamics in the South African Middle Stone Age. Proc. Natl. Acad. Sci. Unit. States Am. 114, 7869e7876.

de Ruiter, D.J., Churchill, S.E., Brophy, J.K., Berger, L.R., 2011. Regional survey of middle stone age fossil vertebrate deposits in the Virginia-Theunissen area of the Free State, South Africa. Navors. Nas. Mus. Bloemfontein 27, 1e20.

Debe,nath, A., Dibble, H.L., 2015. Handbook of Paleolithic Typology: Lower and Middle Paleolithic of Europe. University of Pennsylvania Press.

Dewar, G., Stewart, B.A., 2016. Paleoenvironments, sea levels, and land use in Namaqualand, South Africa, during MIS 6-2. In: Jones, S.C., Stewart, B.A. (Eds.), Africa from MIS 6-2. Springer, Dordrecht, pp. 195e212.

Ecker, M., Brink, J.S., Rossouw, L., Chazan, M., Horwitz, L.K., Lee-Thorp, J.A., 2018. The palaeoecological context of the Oldowan-Acheulean in southern Africa. Nat. Ecol. Evol. 2, 1080e1086.

Ecker, M., Lee-Thorp, J.A., 2018. The dietary ecology of the extinct springbok *Anti- dorcas bondi*. Quat. Int. 495, 136e143.

Ellis, R.P., Vogel, J.C., Fuls, A., 1980. Photosynthetic Pathways and the Geographical Distribution of Grasses in South West Africa/Namibia. South Afr. J. Sci. 76, 307e314.

Farmer, V.C., 1974. The Infrared Spectra of Minerals. Mineralogical Society, London. Galbraith, R.F., Roberts, R.G., Laslett, G.M., Yoshida, H., Olley, J.M., 1999. Optical dating of single and multiple grains of quartz from Jinmium rock shelter, northern Australia: Part I, experimental details and statistical models. Archaeometry 41, 339e364.

Gary, M., McAfee Jr., R., Wolf, C.L., 1972. Glossary of Geology. American Geological Institute, Washington, DC.

Grobler, N.J., Loock, J.C., Behounek, N.J., 1988. Development of pans in paleodrainage in the north-western Orange Free State. Palaeoecol. Afr. Surround. Isl. 19, 87e96.

Grün, R., Brink, J.S., Spooner, N.A., Taylor, L., Stringer, C.B., Franciscus, R.G., Murray, A.S., 1996. Direct dating of Florisbad hominid. Nature 382, 500e501.

Gue,rin, G., Mercier, N., Adamiec, G., 2011. Dose-rate conversion factors: update. Ancient TL 29, 5e8.

Gue,rin, G., Mercier, N., Nathan, R., Adamiec, G., Lefrais, Y., 2012. On the use of the infinite matrix assumption and associated concepts: a critical review. Radiat. Meas. 47, 778e785.

Gue,rin, G., Christophe, C., Philippe, A., Murray, A.S., Thomsen, K.J., Tribolo, C., Urbanova, P., Jain, M., Guibert, P., Mercier, N., Kreutzer, S., Lahaye, C., 2017. Absorbed dose, equivalent dose, measured dose rates, and implications for OSL age estimates: introducing the Average Dose Model. Quat. Geochronol. 41, 163e173.

Haaland, M.M., Czechowski, M., Carpentier, F., Lejay, M., Vandermeulen, B., 2019. Documenting archaeological thin sections in high-resolution: a comparison of methods and discussion of applications. Geoarchaeology 34, 100e114.

Hahn, A., Schefuß, E., Groeneveld, J., Miller, C., Zabel, M., 2021. Glacial to interglacial climate variability in the southeastern African subtropics (25e20° S). Clim. Past 17, 345e360.

Harper, P.T.N., 1997. The Middle Stone Age sequences at Rose Cottage Cave: a search for continuity and discontinuity. South Afr. J. Sci. 93, 470e475.

Henderson, Z., 2001. The integrity of the Middle Stone Age horizon at Florisbad, South Africa. Navors. Nas. Mus. Bloemfontein 17, 25e52.

Henderson, Z., Scott, L., Rossouw, L., Jacobs, Z., 2006. Dating, paleoenvironments, and archaeology: a progress report on the Sunnyside 1 site, Clarens, South Africa. Archaeol. Pap. Am. Anthropol. Assoc. 16, 139e149.

Henshilwood, C.S., d'Errico, F., Yates, R., Jacobs, Z., Tribolo, C., Duller, G.A.T., Mercier, N., Sealy, J.C., Valladas, H., Watts, I., Wintle, A.G., 2002. Emergence of modern human behavior: Middle Stone Age engravings from South Africa. Science 295, 1278e1280.

Henshilwood, C.S., d'Errico, F., van Niekerk, K.L., Coquinot, Y., Jacobs, Z., Lauritzen, S.-E., Menu, M., García-Moreno, R., 2011. A 100,000-year-old ochre- processing workshop at Blombos Cave, South Africa. Science 334, 219e222.

Henshilwood, C.S., Dubreuil, B., 2011. The still Bay and Howiesons Poort, 77-59 ka: symbolic material culture and the evolution of the mind during the African

Middle Stone Age. Curr. Anthropol. 52, 361e400.
Henshilwood, C.S., 2012. Late Pleistocene techno-traditions in southern Africa: a review of the Still Bay and Howiesons Poort, c. 75e59 ka. J. World PreHistory 25, 205e237.
Heydari, M., Gue,rin, G., 2018. OSL signal saturation and dose rate variability: investigating the behaviour of different statistical models. Radiat. Meas. 120, 96e103.
Jacobs, Z., Roberts, R.G., 2017. Single-grain OSL chronologies for the Still Bay and Howieson's Poort industries and the transition between them: further analyses and statistical modelling. J. Hum. Evol. 107, 1e13.
Katz, O., Cabanes, D., Weiner, S., Maeir, A.M., Boaretto, E., Shahack-Gross, R., 2010. Rapid phytolith extraction for analysis of phytolith concentrations and assem- blages during an excavation: an application at Tell es-Safi/Gath, Israel. J. Archaeol. Sci. 37, 1557e1563.
Kent, S., Scholtz, N., 2003. Perspectives on the geology of an open-air Middle Stone Age site, eastern Free State, South Africa. South Afr. J. Sci. 99, 422e424.
King, L.C., 1963. South African Scenery: A Textbook of Geomorphology, third ed.
Klein, R.G., 1994. The long-horned African buffalo (*Pelorovis antiquus*) is an extinct species. J. Archaeol. Sci. 21, 725e733.
Kuman, K., Inbar, M., Clarke, R.J., 1999. Palaeoenvironments and cultural sequence of the Florisbad Middle Stone Age hominid site, South Africa. J. Archaeol. Sci. 26, 1409e1425.
Lacruz, R., Brink, J.S., Hancox, P.J., Skinner, A.R., Herries, A.I.R., Schmid, P., Berger, L.R., 2002. Palaeontology and geological context of a Middle Pleistocene faunal assemblage from the Gladysvale Cave, South Africa. Palaeontol. Afr. 38, 99e114. Lennox, S., Wadley, L., 2022. Middle Stone Age wood use in Rose Cottage Cave South Africa: evidence from charcoal identifications. Quat. Int. 611e612, 102e114.
Lisiecki, L.E., Raymo, M.E., 2005. A Pliocene-Pleistocene stack of 57 globally distributed benthic $\delta^{18}O$ records. Paleoceanography 20.
Lombard, M., 2007. The gripping nature of ochre: the association of ochre with Howiesons Poort adhesives and Later Stone Age mastics from South Africa. J. Hum. Evol. 53, 406e419.
Lombard, M., Phillipson, L., 2010. Indications of bow and stone-tipped arrow use 64 000 years ago in KwaZulu-Natal, South Africa. Antiquity 84, 635e648.
Loock, J.C., Grobler, N.J., 1988. The regional geology of Florisbad. Navors. Nas. Mus. Bloemfontein 5, 489e497.
Lukich, V., Porat, N., Faershtein, G., Cowling, S., Chazan, M., 2019. New chronology and stratigraphy for Kathu Pan 6, South Africa. J. Paleol. Archaeol. 2, 265, 257. Lukich, V., Cowling, S., Chazan, M., 2020. Palaeoenvironmental reconstruction of Kathu Pan, South Africa, based on sedimentological data. Quat. Sci. Rev. 230, 106153.
Lukich, V., Ecker, M., 2022. Pleistocene environments in the southern Kalahari of South Africa. Quat. Int. 614, 50e58.
Lyons, R., Tooth, S., Duller, G.A.T., 2014. Late Quaternary climatic changes revealed by luminescence dating, mineral magnetism and diffuse reflectance spectros- copy of river terrace palaeosols: a new form of geoproxy data for the southern African interior. Quat. Sci. Rev. 95, 43e59.
Mackay, A., Stewart, B.A., Chase, B.M., 2014. Coalescence and fragmentation in the late Pleistocene archaeology of southernmost Africa. J. Hum. Evol. 72, 26e51.
Macphail, R.I., Goldberg, P., 2017. Applied Soils and Micromorphology in Archae- ology. Cambridge University Press, Cambridge.
Marshall, T.R., Harmse, J.T., 1992. A review of the origin and propagation of pans. South Afr. Geogr. 19, 9e21.
Mason, R.J., 1969. Prehistory of the Transvaal. Witwatersrand University Press, Johannesburg.
Mejdahl, V., Bøtter-Jensen, L., 1994. Luminescence dating of archaeological mate- rials using a new technique based on single aliquot measurements. Quat. Sci. Rev. 13, 551e554.
Mohale, N.E., Codron, D., Horwitz, L.K., 2022. Stable isotope evidence for mid- Pleistocene paleoenvironmental conditions at the site of Kathu Pan 1 (central interior, South Africa). Quat. Int. 614, 37e49.
Morris, S.E., 2019. Paleolandscape Reconstruction Using Geoproxy Evidence at Erfkroon, South Africa. Unpublished MA thesis, San Marcos.
Mourre, V., Villa, P., Henshilwood, C.S., 2010. Early use of pressure flaking on lithic artifacts at Blombos Cave, South Africa. Science 330, 659e662.
Mucina, L., Rutherford, M.C., 2006. The Vegetation of South Africa, Lesotho and Swaziland. South African National Biodiversity Institute, Pretoria.
Mulholland, S.C., Rapp, G.J., 1992. Phytolith Systematics. Emerging Issues. Plenum Press, New York.
Murray, A.S., Wintle, A.G., 2000. Luminescence dating of quartz using an improved single-aliquot regenerative-dose protocol. Radiat. Meas. 32, 57e73.
Nathan, R.P., Mauz, B., 2008. On the dose-rate estimate of carbonate-rich sediments for trapped charge dating. Radiat. Meas. 43, 14e25.
Neumann, K., Stro€mberg, C.A.E., Ball, T., Albert, R.M., Vrydaghs, L., Scott Cummings, L., 2019. International Code for Phytolith Nomenclature (ICPN) 2.0. Ann. Bot. 124, 189e199.
Partridge, T.C., deMenocal, P.B., Lorentz, S.A., Paiker, M.J., Vogel, J.C., 1998. Orbital forcing of climate over South Africa: a 200,000-year rainfall record from the Pretoria saltpan. Quat. Sci. Rev. 116, 1125e1133.
Pazan, K.R., Dewar, G., Stewart, B.A., 2022. The MIS 5a (~80 ka) Middle Stone Age lithic assemblages from Melikane Rockshelter, Lesotho: highland adaptation and social fragmentation. Quat. Int. 611e612, 115e133.
Philippe, A., Gue,rin, G., Kreutzer, S., 2019. BayLum - an R package for Bayesian analysis of OSL ages: an introduction. Quat. Geochronol. 49, 16e24.
Pienaar, M., Woodborne, S., Wadley, L., 2008. Optically stimulated luminescence dating at Rose Cottage Cave. South Afr. J. Sci. 104, 65e70.
Piperno, D.R., 2006. Phytoliths: A Comprehensive Guide for Archaeologists and Paleoecologists. AltaMira Press, Lanham, MD.
Plug, I., 1988. Hunters and Herders: an Archaeozoological Study of Prehistoric Communities in the Kruger National Park. Unpublished PhD thesis. University of Pretoria.
Prescott, J.R., Hutton, J.T., 1994. Cosmic ray contributions to dose rates for lumi- nescence and ESR dating: large depths and long-term time variations. Radiat. Meas. 23, 497e500.
Robbins, L.H., Brook, G.A., Murphy, M.L., Ivester, A.H., Campbell, A.C., 2016. The Kalahari during MIS 6-2 (190-12 ka): archaeology, paleoenvironment, and population dynamics. In: Jones, S.C., Stewart, B.A. (Eds.), Africa from MIS 6-2. Springer, Dordrecht, pp. 175e194.
Rossouw, L., 2006. Florisian mammal fossils from erosional gullies along the Modder River at Mitasrust farm, central Free State, South Africa. Navors. Nas. Mus. Bloemfontein 22, 145e161.
Rossouw, L., 2009. The Application of Fossil Grass-Phytolith Analysis in the Reconstruction of Cainozoic Environments in the South African Interior. Un- published PhD thesis. University of the Free State, Bloemfontein, South Africa. Rossouw, L., 2016. An Early Pleistocene phytolith record from Wonderwerk cave, northern Cape, South Africa. Afr. Archaeol. Rev. 33, 251e263.
Russell-Gibbs, G.E., Watson, L., Koekemoer, M., Smook, L., Barker, N.P., Anderson, H.M., Dallwitz, M.J., 1990. Grasses of Southern Africa. National Botanical Institute.
Sampson, C.G., 1968. The Middle Stone Age Industries of the Orange River Scheme Area. National Museum, Bloemfontein.
Sampson, C.G., Moore, V., Bousman, C.B., Stafford, B., Giordano, A., Willis, M., 2015. A GIS analysis of the Zeekoe Valley Stone Age archaeological record in South Africa. J. Afr. Archaeol. 13, 167e185.
Schmidt, P., Porraz, G., Slodczyk, A., Bellot-Gurlet, L., Archer, W., Miller, C.E., 2013. Heat treatment in the South African Middle Stone Age: temperature induced transformations of silcrete and their technological implications. J. Archaeol. Sci. 40, 3519e3531.
Schulze, E.-D., Ellis, R., Schulze, W., Trimborn, P., Ziegler, H., 1996. Diversity, meta- bolic types and $\delta^{13}C$ carbon isotope ratios in the grass flora of Namibia in relation to growth form, precipitation and habitat conditions. Oecologia 106, 352e369.
Scott, L., Rossouw, L., 2005. Reassessment of botanical evidence for palae- oenvironments at Florisbad, South Africa. S. Afr. Archaeol. Bull. 60, 96e102.
Scott, L., 2016. Fluctuations of vegetation and climate over the last 75 000 years in the Savanna Biome, South Africa: Tswaing Crater and Wonderkrater pollen sequences reviewed. Quat. Sci. Rev. 145, 117e133.
Scott, L., Neumann, F.H., 2018. Pollen-interpreted palaeoenvironments associated with the Middle and Late Pleistocene peopling of southern Africa. Quat. Int. 495, 169e184.
Scott, L., van Aardt, A.C., Brink, J.S., Toffolo, M.B., Ochando, J., Carrio,n, J.S., 2019. Palynology of Middle Stone Age spring deposits in grassland at the Florisbad hominin site, South Africa. Rev. Palaeobot. Palynol. 265, 13e26.
Scott, L., Sobol, M., Neumann, F.H., Gil Romera, G., Fern,andez-Jalvo, Y., Bousman, C.B., Horwitz, L.K., van Aardt, A.C., 2022. Late Quaternary palae- oenvironments in the central semi-arid region of South Africa from pollen in cave, pan, spring, stream and dung deposits. Quat. Int. 614, 84e97.
Sealy, J., 2016. Cultural change, demography, and the archaeology of the last 100 kyr in southern Africa. In: Jones, S.C., Stewart, B.A. (Eds.), Africa from MIS 6-2. Springer, Dordrecht, pp. 65e76.
Soriano, S., Villa, P., Wadley, L., 2007. Blade technology and tool forms in the Middle Stone Age of South Africa: the Howiesons Poort and post-Howiesons Poort at Rose Cottage Cave. J. Archaeol. Sci. 34, 681e703.
Soriano, S., Villa, P., Delagnes, A., Degano, I., Pollarolo, L., Lucejko, J.J., Henshilwood, C., Wadley, L., 2015. The Still Bay and Howiesons Poort at Sibudu and Blombos: understanding Middle Stone Age technologies. PLoS One 10, e0131127.
Steele, T.E., Mackay, A., Fitzsimmons, K.E., Igreja, M., Marwick, B., Orton, J., Schwortz, S., Stahlschmidt, M.C., 2016. Varsche Rivier 003: a Middle and Later Stone Age site with Still Bay and Howiesons Poort assemblages in southern Namaqualand, South Africa. PaleoAnthropology 100e163.
Stewart, B.A., Dewar, G.I., Morley, M.W., Inglis, R.H., Wheeler, M., Jacobs, Z., Roberts, R.G., 2012. Afromontane foragers of the Late Pleistocene: site forma- tion, chronology and occupational pulsing at Melikane Rockshelter, Lesotho. Quat. Int. 270, 40e60.
Stewart, B.A., Parker, A.G., Dewar, G., Morley, M.W., Allott, L.F., 2016. Follow the Senqu: Maloti-Drakensberg paleoenvironments and implications for early hu- man dispersals into mountain systems. In: Jones, S.C., Stewart, B.A. (Eds.), Africa from MIS 6-2. Springer, Dordrecht, pp. 247e272.
Stoops, G., Marcelino, V., Mees, F., 2018. Interpretation of Micromorphological Features of Soils and Regoliths, second ed. Elsevier, Oxford.
Stoops, G., 2021. Guidelines for Analysis and Description of Soil and Regolith Thin Sections, second ed. Wiley.
Stro€mberg, C.A.E., 2004. Using phytolith assemblages to reconstruct the origin and spread of grass-dominated habitats in the great plains of North America during the late Eocene to early Miocene. Palaeogeogr. Palaeoclimatol. Palaeoecol. 207, 239e275.
Telfer, M.W., Thomas, D.S.G., 2007. Late Quaternary linear dune accumulation and chronostratigraphy of the southwestern Kalahari: implications for aeolian palaeoclimatic reconstructions and predictions of future dynamics. Quat. Sci.

Rev. 26, 2617e2630.
Texier, P.-J., Porraz, G., Parkington, J., Rigaud, J.-P., Poggenpoel, C., Miller, C., Tribolo, C., Cartwright, C., Coudenneau, A., Klein, R., Steele, T., Verna, C., 2010. A Howiesons Poort tradition of engraving ostrich eggshell containers dated to 60,000 years ago at Diepkloof Rock Shelter, South Africa. Proc. Natl. Acad. Sci. Unit. States Am. 107, 6180.
Toffolo, M.B., Brink, J.S., Berna, F., 2015. Bone diagenesis at the Florisbad spring site, Free State Province (South Africa): implications for the taphonomy of the Middle and Late Pleistocene faunal assemblages. J. Archaeol. Sci.: Report 4, 152e163.
Toffolo, M.B., Brink, J.S., van Huyssteen, C., Berna, F., 2017. A microstratigraphic reevaluation of the Florisbad spring site, Free State Province, South Africa: formation processes and paleoenvironment. Geoarchaeology 32, 456e478.
Toffolo, M.B., Brink, J.S., Berna, F., 2019a. Microstratigraphic reconstruction of for- mation processes and paleoenvironments at the Early Pleistocene Cornelia- Uitzoek hominin site, Free State Province, South Africa. J. Archaeol. Sci.: Report 25, 25e39.
Toffolo, M.B., Regev, L., Dubernet, S., Lefrais, Y., Boaretto, E., 2019b. FTIR-based crystallinity assessment of aragoniteecalcite mixtures in archaeological lime binders altered by diagenesis. Minerals 9.
Toffolo, M.B., 2021. The significance of aragonite in the interpretation of the microscopic archaeological record. Geoarchaeology 36, 149e169.
Tooth, S., Hancox, J.P., Brandt, D., McCarthy, T.S., Jacobs, Z., Woodborne, S., 2013. Controls on the genesis, sedimentary architecture, and preservation potential of the dryland alluvial successions in stable continental interiors: insights from the incising Modder River, South Africa. J. Sediment. Res. 83, 541e561.
Tribolo, C., Mercier, N., Douville, E., Joron, J.-L., Reyss, J.-L., Rufer, D., Cantin, N., Lefrais, Y., Miller, C.E., Porraz, G., Parkington, J., Rigaud, J.-P., Texier, P.-J., 2013. OSL and TL dating of the Middle Stone Age sequence at Diepkloof Rock Shelter (South Africa): a clarification. J. Archaeol. Sci. 40, 3401e3411.
Tribolo, C., Mercier, N., Loïc, N., Taffin, N., Miller, C.E., Will, M., Conard, N.J., 2022. Luminescence dating estimates for the coastal MSA sequence of Hoedjiespunt 1 (South Africa). J. Archaeol. Sci.: Report 41, 103320.
Trower, G., 2010. An Investigation into the Archaeological, Palaeontological and Stratigraphic Continuity between Two Sections of the Free State's Modder River, Observed within Selected Erosional Gullies (Dongas). Unpublished M.Sc. thesis. University of the Free State.
Twiss, P.C., Suess, E., Smith, R.M., 1969. Morphological classification of grass phy- toliths. Soil Sci. Soc. Am. 33, 109e115.
Urrego, D.H., Sa¸nchez Gon~i, M.F., Daniau, A.L., Lechevrel, S., Hanquiez, V., 2015. Increased aridity in southwestern Africa during the warmest periods of the last interglacial. Clim. Past 11, 1417e1431.
Valladas, H., Wadley, L., Mercier, N., Froget, L., Tribolo, C., Reyss, J.-L., Joron, J.L., 2005. Thermoluminescence dating of burnt lithics from middle stone age layers at Rose Cottage Cave. South Afr. J. Sci. 101, 169e174.
van Aardt, A.C., Bousman, C.B., Brink, J.S., Brook, G.A., Jacobs, Z., du Preez, P.J., Rossouw, L., Scott, L., 2016. First chronological, palaeoenvironmental, and archaeological data from the Baden-Baden fossil spring complex in the western Free State, South Africa. Palaeoecol. Afr. 33, 117e152.
Van Couvering, J.A., Delson, E., 2020. African Land Mammal Ages. J. Vertebr. Pale- ontol. 40, e1803340.
van der Marel, H.W., Beutelspacher, H., 1976. Atlas of Infrared Spectroscopy of Clay Minerals and Their Admixtures. Elsevier Scientific Publishing Company, Amsterdam.
van Hoepen, E.C.N., 1932. Die Mosselbaaise Kultuur. In: Argeologiese Navorsing van die Nasionale Museum Bloemfontein, 1, pp. 27e54.
van Riet Lowe, C., 1931. A Rare Point from Sheppard Island, vol. 20. Transactions of the Royal Society of South Africa, pp. 57e58.
Vepraskas, M.J., Lindbo, D.L., Stolt, M.H., 2018. Redoximorphic features. In: Stoops, G., Marcelino, V., Mees, F. (Eds.), Interpretation of Micromorphological Features of Soils and Regoliths, second ed. Elsevier, Oxford, pp. 425e446.
Villa, P., Soressi, M., Henshilwood, C.S., Mourre, V., 2009. The Still Bay points of Blombos Cave (South Africa). J. Archaeol. Sci. 36, 441e460.
Vogel, J.C., Fuls, A., Ellis, R.P., 1978. The geographical distribution of Kranz grasses in South Africa. South Afr. J. Sci. 74, 209e215.
von den Driesch, A., 1976. A Guide to the Measurement of Animal Bone from Archaeological Sites. Peabody Museum Press, Cambridge.
Wadley, L., Hodgskiss, T., Grant, M., 2009. Implications for complex cognition from the hafting of tools with compound adhesives in the Middle Stone Age, South Africa. Proc. Natl. Acad. Sci. Unit. States Am. 106, 9590e9594.
Wadley, L., 2013. Recognizing complex cognition through innovative technology in Stone Age and Palaeolithic sites. Camb. Archaeol. J. 23, 163.
Wadley, L., 2015. Those marvellous millennia: the Middle Stone Age of southern Africa. Azania 50, 155e226.
Weiner, S., 2010. Microarchaeology. Beyond the Visible Archaeological Record. Cambridge University Press, New York.
Wells, L.H., Cooke, H.B.S., Malan, B.D., 1942. The associated fauna and culture of the Vlakkraal Thermal Springs. O.F.S. Trans. Roy. Soc. S. Afr. 29, 203e233.
Wilkins, J., Schoville, B.J., Brown, K.S., Gliganic, L., Meyer, M.C., Loftus, E., Pickering, R., Collins, B., Blackwood, A.F., Makalima, S., Hatton, A., Maape, S., 2020. Fabric Analysis and Chronology at Ga-Mohana Hill North Rockshelter, Southern Kalahari Basin: Evidence for In Situ, Stratified Middle and Later Stone Age Deposits. J. Paleol. Archaeol. 3, 336e361.
Wilkins, J., Schoville, B.J., Pickering, R., Gliganic, L., Collins, B., Brown, K.S., von der Meden, J., Khumalo, W., Meyer, M.C., Maape, S., Blackwood, A.F., Hatton, A., 2021. Innovative *Homo sapiens* behaviours 105,000 years ago in a wetter Kalahari. Nature 592, 248e252.
Woillez, M.N., Levavasseur, G., Daniau, A.L., Kageyama, M., Urrego, D.H., Sa¸nchez-Gon~i, M.F., Hanquiez, V., 2014. Impact of precession on the climate, vegetation and fire activity in southern Africa during MIS 4. Clim. Past 10, 1165e1182.
Wurz, S., 2016. Development of the archaeological record during the Middle Stone Age of South Africa. In: Knight, J., Grab, S.W. (Eds.), Quaternary Environmental Change in Southern Africa: Physical and Human Dimensions. Cambridge Uni- versity Press, Cambridge, pp. 371e384.
Ziegler, M., Simon, M.H., Hall, I.R., Barker, S., Stringer, C., Zahn, R., 2013. Develop- ment of Middle Stone Age innovation linked to rapid climate change. Nat. Commun. 4, 1905.